nature mental health

Article

https://doi.org/10.1038/s44220-024-00377-0

Brain dynamics reflecting an intra-network brain state are associated with increased post-traumatic stress symptoms in the early aftermath of trauma

Received: 1 March 2024

Accepted: 5 December 2024

Published online: 20 January 2025

Check for updates

A list of authors and their affiliations appears at the end of the paper

Post-traumatic stress (PTS) encompasses a range of psychological responses following trauma, which may lead to more severe outcomes such as post-traumatic-stress disorder (PTSD). Identifying early neuroimaging biomarkers that link brain function to PTS outcomes is critical for understanding PTSD risk. This longitudinal study examines the association between brain dynamic functional network connectivity and current/future PTS symptom severity, and the impact of sex on this relationship. By analyzing 275 participants' dynamic functional network connectivity data obtained ~2 weeks after trauma exposure, we noted that brain dynamics of an inter-network brain state link negatively with current ($r = -0.197$, $P_{corrected} = 0.0079$) and future ($r = -0.176$, $P_{corrected} = 0.0176$) PTS symptom severity. In addition, dynamics of an intra-network brain state correlated with future symptom intensity ($r = 0.205$, $P_{corrected} = 0.0079$). We additionally observed that the association between the network dynamics of the inter-network and intra-network brain state with symptom severity is more pronounced in the female group. Our findings highlight a potential link between brain network dynamics in the aftermath of trauma with current and future PTSD outcomes, with a stronger effect in the female group, underscoring the importance of sex differences.

Post-traumatic-stress disorder (PTSD) may develop in individuals who have experienced or witnessed a traumatic event, such as military warfare, sexual or physical assault, accidents or natural disasters[1]. Symptoms of PTSD include distressing thoughts, flashbacks, avoidance of reminders, changes in mood and cognition, and increased arousal, which can impact an individual's life[2]. Biological markers, or biomarkers, may be able to identify those who are more likely to develop PTSD following a traumatic incident[3,4]. Early identification of such individuals might allow for prompt treatment and preventive measures, potentially minimizing the severity and duration of PTSD symptoms. Furthermore, these markers may help in the development of tailored treatment methods, the optimization of therapeutic treatments and the long-term monitoring of therapy response[5]. .

In recent years, there has been a significant increase in the exploration and advancement of neuroimaging-based markers for identifying vulnerability to PTSD[6,7]. This emerging field shows great potential in the rapid development of tools for early identification and intervention[8]. Studies utilizing neuroimaging techniques have uncovered notable alterations in brain function among individuals with PTSD. These alterations are marked by atypical functional network connectivity (FNC) patterns, as observed in resting-state functional magnetic resonance imaging (fMRI) studies[9–11]. Specifically, these patterns are seen in various brain regions, including the hippocampus[12], amygdala[13],

e-mail: msendi@mclean.harvard.edu

visual network[14] and prefrontal cortex[13] in individuals with PTSD. This underscores the extensive influence of trauma on brain networks. Furthermore, several studies have successfully utilized resting-state fMRI functional connectivity to predict the severity of PTSD symptoms[15–18]. In addition, two recent studies revealed the ability to predict future symptom severity in participants with PTSD by analyzing resting-state fMRI data obtained after the trauma had occurred[19,20].

It has been assumed that brain FNC remains quasi-static or invariant over long periods, leading many previous studies to focus solely on static FNC (sFNC) while ignoring the brain dynamics during rest. However, challenging this assumption, a relatively new concept called dynamic FNC (dFNC) has emerged[21–25]. A dynamic approach recognizes that FNC during the relatively short length of resting-state fMRI scans can exhibit temporal variations, thereby highlighting the importance of studying the dynamic aspects of FNC[26]. Unlike sFNC, dFNC offers greater sensitivity in capturing the spontaneous adaptations that occur in response to various cognitive and mental conditions[27]. By considering the spontaneously fluctuating nature of neural signals across different temporal scales, dFNC allows for a more sophisticated evaluation of brain activity [28].

Considering the dynamic nature of FNC in resting-state fMRI, several studies have explored dFNC in the context of PTSD in recent years[29–32]. However, none of these studies has examined the capability of dFNC to link with the future PTSD symptom severity. In addition, previous research indicates that women are two to three times more likely than men to develop PTSD[33]. Despite this, there has been a notable absence of studies that examine the potential effects of sex on the relationship between dFNC variables and the severity of current or future PTSD symptoms.

In the present study, we aim to build on previous research on dFNC in the context of PTSD. Specifically, we investigated the link between dFNC variables and future PTSD symptom severity. In addition, we explored the potential effects of sex on the association between dFNC variables and both current and future symptom severity. As past studies have demonstrated, biological sex is not the primary determinant of the various neurophenotypes associated with adverse post-traumatic outcomes. Instead, a range of other factors such as low socioeconomic status, including income[34,35], housing quality[36] and broader socioeconomic conditions, area deprivation index (ADI)[37], also significantly influence the risk and severity of PTSD. To address the contribution of these factors, we also included them as covariates in our analysis. Finally, our study aimed to identify specific brain states that underlie risk and protective mechanisms related to PTSD.

To accomplish these goals, we utilized the dataset from the Advancing Understanding of Recovery after Trauma (AURORA) project[38]. In the AURORA study, understanding whether dFNC variables derived from resting-state fMRI early after a trauma can link with future PTSD symptom severity is crucial. This is especially true since neuroimaging was conducted approximately 2 weeks after the traumatic event, at a time when acute stress disorder may be assessed but before the diagnosis of PTSD can be made. This timing allows us to investigate the potential of dFNC variables as early biomarkers for PTSD and evaluate their predictive capability for the severity of PTSD symptoms at a later stage.

Results

Participants

Data for the current analyses were collected as part of the multisite emergency department (ED) AURORA study. The AURORA study represents a significant research effort aimed at enhancing our understanding, prevention and recovery strategies for individuals who have undergone a traumatic event. In the AURORA study, trauma-exposed civilians brought to one of 29 participating EDs across the United States were recruited for this large, longitudinal study (details in ref. 38). This study involved around 3,000 participants from the AURORA project, who provided clinical data at various intervals following the trauma: 2 weeks (WK2), 4 weeks (WK4), 3 months (M3), 6 months (M6) and 12 months (M12) as illustrated in Fig. 1a. In addition, neuroimaging data from ~400 participants were collected at WK2 from five different scanning locations: Atlanta (Georgia), Belmont (Massachusetts), Philadelphia (Pennsylvania), St Louis (Missouri) and Detroit (Michigan). The recruitment for this study took place between September 2017 and June 2021 (Final freeze 4 Psychometric release at 22 September 2021). We excluded those with low-quality resting-state fMRI and missing clinical information at the imaging acquisition date. This process resulted in 275 participants (181 female participants) being included in this analysis. Table 1 presents the demographic characteristics of the participants included in this study. In addition, Supplementary Fig. 1 illustrates the distribution of the PTSD Checklist for the *Diagnostic and Statistical Manual of Mental Disorders* 5th Edition (PCL-5)[39] scores at various time points for the participants.

Three distinct dFNC states were identified

After calculating the dFNC of each participant, we grouped their dFNC into three different dynamic network connectivity states (Fig. 1c). Figure 2 presents an overview of the identified states. Each state represents 1,378 connectivity measures among 7 networks across the entire brain (Fig. 1b): the subcortical network (SCN), auditory network (ADN), sensorimotor network (SMN), visual network (VSN), cognitive control network (CCN), default-mode network (DMN) and cerebellar network (CBN). The top panel highlights three distinct dFNC states, while the bottom panel shows the data with connectivities between −0.3 and 0.3 removed for clarity. State 2 and state 3 exhibit a stronger positive connectivity among sensory networks, including visual, auditory and sensorimotor networks. Conversely, in state 1, we observed more disconnections among these networks. We observed an increase in within-CCN connectivity and enhanced connectivity between the DMN and sensory networks in state 3. In addition, we noted a greater connectivity between the CBN and SCN in state 3 compared with the other two states. Overall, our analysis suggests that state 2 and state 3 exhibit characteristics of inter-network states, evidenced by the increased connectivity across the seven networks. By contrast, state 1 is indicative of an intra-network state as it demonstrates predominantly within-network connectivity

Fig. 1 | Data collection procedure and analytic pipeline. a, The PCL-5 was utilized to evaluate PTSD symptoms at various time points, encompassing pre-trauma (PRE), WK2, WK8, (M3, M6 and M12. During the study visit at WK2, a subgroup of participants underwent MRI scans, in either the morning or the afternoon. **b**, We utilized the NeuroMark pipeline to extract robust intrinsic connectivity networks (ICNs), totaling 53 components, which demonstrate consistent replication across independent datasets. These 53 distinct components were initially identified through group independent component analysis using the NeuroMark template. In this figure, *X*, *Y* and *Z* represent the Montreal Neurological Institute (MNI) coordinates. These components were subsequently categorized into seven distinct networks: the SCN, ADN, VSN, SMN, CCN, DMN and CBN. **c**, The dFNC analytic pipeline. Step 1: initially, the time-course signal of 53 ICNs was identified through group independent component analysis in the Neuromark template. Subsequently, the identified 53 ICNs were subjected to a taper sliding window segmentation to calculate FNC. Each participant yielded 210 FNCs, each with a size of 53 × 53. Step 2: to cluster the FNCs into three distinct groups, the FNC matrices were vectorized and concatenated, followed by the utilization of k-means clustering with correlation as the distance metric. Step 3: from the state vector, OCR was computed for each participant, resulting in a total of three OCR variables for each participant. To investigate the relationship between OCRs with the PTSD clinical measure (PCL-5), we used GLM to compute the associations, taking into account factors such as age, sex, years of education, scanning site, income, marital status, employment status, type of trauma and percentile ADI. The resulting *t* statistics from this analysis were then converted to correlation (*r*) values.

https://doi.org/10.1038/s44220-024-00377-0

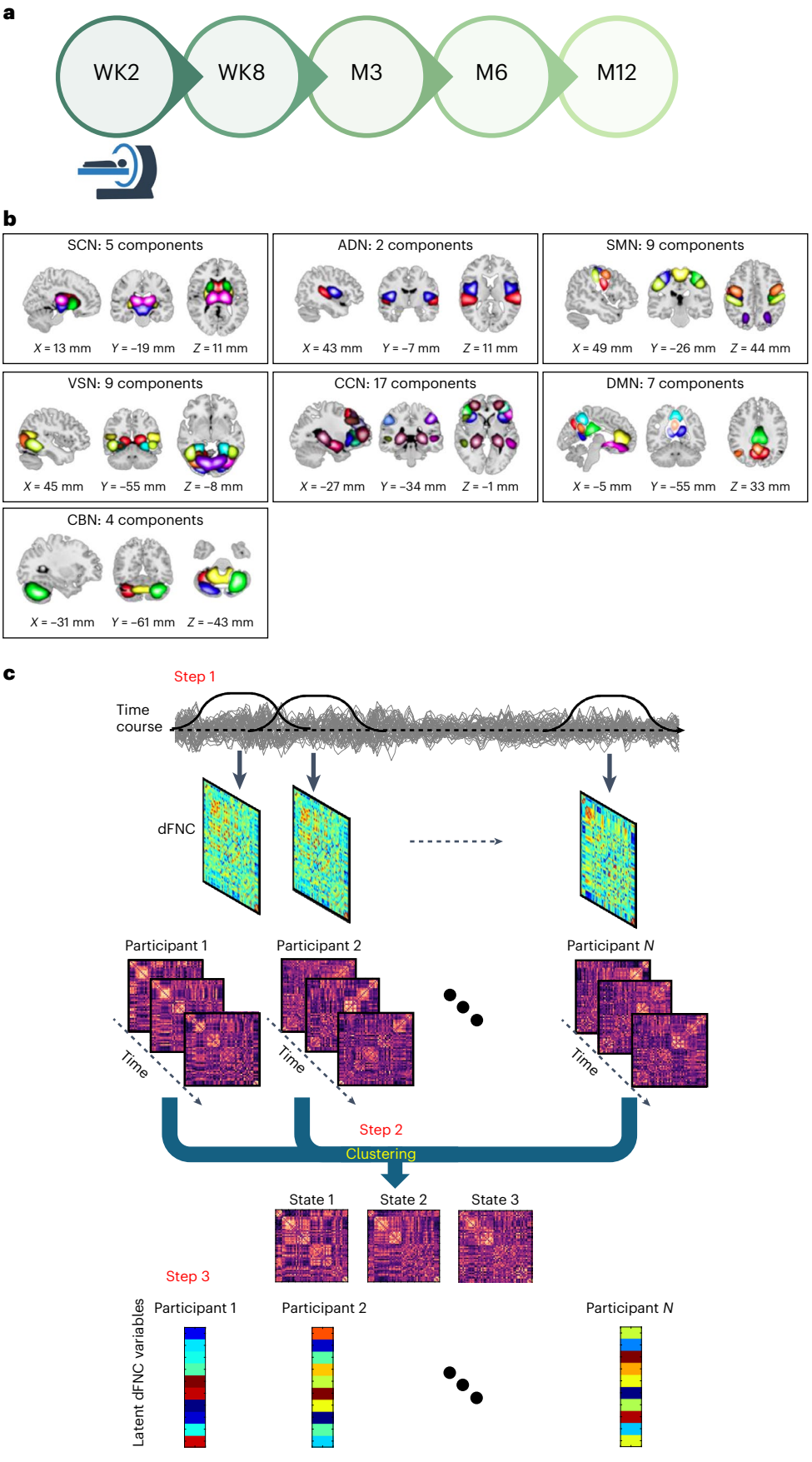

Table 1 | Participant demographics and clinical information

Characteristic	Mean (s.d.) or *N* (%)
Demographic characteristic	
Age	34.55 (12.78)
Sex assigned at birth, male/female	94 (34.18%)/181 (65.82%)
Race/ethnicity[a]	
Hispanic	42 (15.27%)
White	85 (30.91%)
Black	131 (47.64%)
Others	15 (5.45%)
Missing	2 (0.73%)
Years of education	15.16 (2.31)
Income level	
<$19,000	74 (26.91%)
$19,001–$35,000	85 (30.91%)
$35,001–$50,000	40 (14.55%)
$50,001–$75,000	30 (10.91%)
$75,001–$100,000	17 (6.18%)
>$100,000	20 (7.27%)
Missing	9 (3.27%)
Trauma type	
Motor vehicle collision	197 (71.64%)
Physical assault	29 (10.55%)
Fall of <10 feet or from unknown height	14 (5.09%)
Non-motorized collision	11 (4%)
Animal-related	7 (2.55%)
Fall of ≥10 feet	4 (1.45%)
Sexual assault	2 (0.73%)
Burns	1 (0.36%)
Incident causing traumatic stress exposure to many people	1 (0.36%)
Poisoning[b]	0 (0%)
Other	9 (3.27%)
Clinical characteristic	
PCL-5 score	
WK2 (*N*=275)	30.12 (17.58)
WK8 (*N*=243)	26.60 (17.30)
M3 (*N*=226)	23.53 (17.40)
M6 (*N*=208)	21.00 (17.33)
M12 (*N*=176)	20.33 (17.93)

[a]Self-reported. [b]None of the participants involved in this study experienced poisoning trauma, although poisoning has been reported as a type of trauma in the broader AURORA group, accounting for around 2% of cases.

patterns. Supplementary Fig. 2 provides further insights into the differences in FNC between states.

Dynamic FNC occupancy rates link with PCL-5 scores

By utilizing the three identified brain states for the entire group and the state vector, estimated for each individual, which represents the state of the brain network at any given time point, we calculated three occupancy rates (OCRs) for each participant. The OCR of each state represents the proportion of time each participant spends in that state (Methods and Supplementary Fig. 3). Figure 3 shows the correlation between OCRs and PCL-5 scores at various time points. The associations were computed using general linear model (GLM) accounting for age, sex, years of education, scanning site, income, marital status, employment status, type of trauma, and percentile ADI, and the resulting *t* statistics were transformed to correlation (*r*). As shown in Fig. 3a, a positive significant association was found between the OCR of state 1 and the PCL-5 scores at M3 ($r = 0.205$, $\beta = 0.0042$, standard error (SE) = 0.0012, 95% confidence interval (CI): ~0.0018–0.0066, $P_{corrected} = 0.0079$, $N = 226$ after excluding sample with missing scores; Table 1). These results indicate that the participants with higher PTSD symptom severity spend more time in state 1, which is indicative of an intra-network brain state.

We observed significant negative association between the OCR of state 3 and the PCL-5 scores at WK2 ($r = -0.197$, $\beta = -0.0033$, SE = 0.0009, 95% CI: ~−0.0052 to −0.0013, $P_{corrected} = 0.0079$, $N = 275$). We also found a negative correlation between state 3 OCR and PCL-5 of M3 ($r = -0.176$, $\beta = -0.0032$, SE = 0.0011, 95% CI: ~−0.0054 to −0.0011, $P_{corrected} = 0.0176$, $N = 226$). This indicates that individuals with higher PCL-5 scores spent less time in state 3, which is indicative of an inter-network brain state. Overall, our findings highlight the relationships between the OCR and PCL-5 scores, suggesting potential connections between dFNC variables and symptoms of PTSD at different time points after trauma.

Sex modulates OCRs and PCL-5 scores relationship

To examine the influence of sex on the relationship between OCRs and PCL-5 scores, we conducted GLM analyses for male ($N = 94$) and female ($N = 181$) participants separately. In these analyses, we included age, years of education, scanning site, income, marital status, employment status, type of trauma and percentile ADI as covariates. The correlation results between OCRs and PCL-5 scores for female and male groups are presented in Fig. 3b and Fig. 3c, respectively. While no significant association was found between OCRs and PCL-5 scores in the male group, we did observe significant associations between the OCRs of state 1 and state 3 with PCL-5 scores at WK2 and M3 in the female group. We observed a positive association between the OCR of state 1 and PCL-5 scores at WK2 ($r = 0.187$, $\beta = 0.0034$, SE = 0.0014, 95% CI: ~0.0001–0.0045, $P_{corrected} = 0.044$, $N = 181$) and M3 ($r = 0.224$, $\beta = 0.0044$, SE = 0.0014, 95% CI: ~0.0018–0.0066, $P_{corrected} = 0.019$, $N = 154$). We also identified a negative correlation between the OCR of state 3 and PCL-5 scores at WK2 ($r = -0.269$, $\beta = -0.0043$, SE= 0.0011, 95% CI: ~−0.0052 to −0.0013, $P_{corrected} = 0.004$, $N = 181$) and M3 ($r = -0.208$, $\beta = -0.0036$, SE= 0.0013, 95% CI: ~−0.0055 to −0.0011, $P_{corrected} = 0.014$, $N = 154$). In addition, the OCR of state 3 showed a negative link with M12 PCL-5 ($r = -0.154$, $\beta = -0.0031$, SE = 0.0015, 95% CI: ~−0.0054–0.0003, $P_{uncorrected} = 0.039$, $N = 117$). However, this link was not significant after false discovery rate (FDR) correction. To confirm that the stronger correlation observed in the female group is not due merely to their larger sample size compared with the male group, we compared the correlations between OCR of state 1 and state 3 with PCL-5 scores at WK2 and M3 for both groups. We employed Fisher's *z* transformation to compare the correlations, calculating the standard errors to ensure precision. Our results indicated a significant difference between female and male groups for the correlation with state 1 OCR (|*Z*-test statistic| = 2.1262, $P = 0.033$), and similarly for state 3 OCR (|*Z*-test statistic| = 2.1029, $P = 0.035$). This suggests that the relationships between OCR of state 1 and state 3 with PCL-5 scores at WK2 are significantly different between the sexes.

PTS and non-PTS groups generate similar dFNC states

We categorized participants into post-traumatic stress (PTS; $N = 124$) and non-PTS ($N = 151$) groups on the basis of their WK2 PCL-5 scores, with a cut-off point of 31. Those scoring above 31 were classified as PTS, while those below were considered non-PTS[39]. We used the term PTS instead of PTSD because the classification was based on PCL-5 scores at the time of imaging (WK2), before an official PTSD diagnosis at WK8.

https://doi.org/10.1038/s44220-024-00377-0

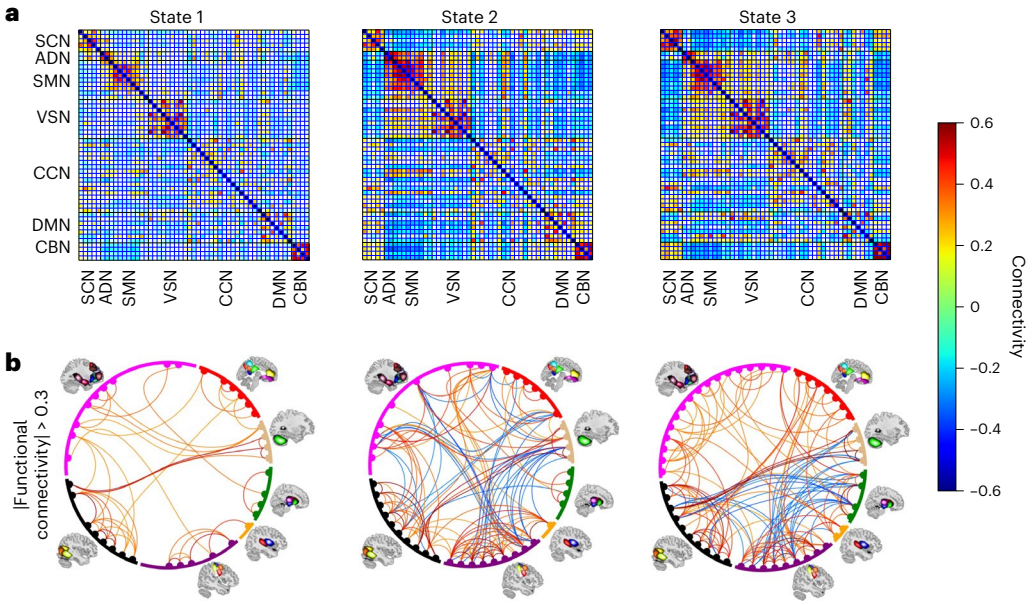

Fig. 2 | Three dFNC states identified in AURORA dataset. a, Three dFNC states identified using k-means clustering method for $N = 275$, including both PTS and non-PTS individuals. **b**, To enhance clarity, the dFNC states are displayed after removing connectivities with values between −0.3 and 0.3. States 2 and 3 exhibit stronger positive connectivity among sensory networks (visual, auditory and sensorimotor). State 1, by contrast, shows more disconnections within these networks. State 3 demonstrates increased within-CCN connectivity and enhanced connectivity between the DMN and sensory networks compared with state 1 and state 2. State 3 also exhibits greater connectivity between the CBN and SCN compared with the other two states. Overall, our analysis identifies states 2 and 3 as inter-network brain states while state 1 appears to be an intra-network brain state according to connectivity patterns. The color bar indicates the strength of the connectivity.

We then examined state pattern differences between the two groups by performing separate k-means clustering analyses on their dFNC data. Figure 4 demonstrates a notable similarity in brain states between the PTS and non-PTS groups, as anticipated. We quantified the similarity by calculating the Pearson correlation coefficient between corresponding states' FNC. The correlations between state 1 of the non-PTS group and state 1 of the PTS group, state 2 of the non-PTS group and state 2 of the PTS group, and state 3 of the non-PTS group and state 3 of the PTS group were 0.9632 ($N = 1{,}378$, where N is number of connections, $P \approx 0$), 0.9880 ($N = 1{,}378$, $P \approx 0$) and 0.8938 ($N = 1378$, $P \approx 0$), respectively (see Fig. 4a,b). The P value, displayed as zero in MATLAB, indicates a very small value, suggesting strong statistical significance and reinforcing the robustness of our findings. Comparing the OCR of states in the non-PTS and PTS groups, we found a consistent pattern: state 1 consistently showed the highest OCR, while state 2 exhibited the lowest OCR in both groups (Fig. 4c,d). These results suggest a consistent OCR pattern across states in both groups, indicating a high degree of similarity in identified brain states between the non-PTS and PTS groups. In addition, our findings that individuals with PTS tend to spend more time in state 1 compared with those without PTS corroborate our main finding that has established a connection between the heightened OCR of this state and PCL-5, hinting at the potential clinical relevance of this brain state in PTS.

Discussion

This research aimed to investigate the significance of temporal changes in brain connectivity, measured by dFNC, in indicating the presence and severity of PTSD symptoms. In addition, we examined the influence of sex-specific differences on the predictive ability of these connectivity measures. Our results indicate that the amount of time spent in an inter-network brain state serves as a protective factor against PTSD, whereas time spent in an intra-network brain state is linked to a higher PTSD symptom severity. Furthermore, we observed that the association between the duration spent in the indentified states and PCL-5 is more pronounced in the female group.

Dynamic FNC offers an enhanced predictive power compared with sFNC, supplying an additional layer of information about the severity of symptoms in brain disorders over time, a level of detail not attainable by its static counterparts[40–42]. For example, a recent study demonstrated that a classification model relying on dFNC variables surpassed the performance of other classification models in patients diagnosed with multiple sclerosis[42]. In another study involving participants with PTSD, the temporal variability, as captured by dFNC, demonstrated a higher classification accuracy than the model obtained only by sFNC variables[41]. Our findings extend beyond previous dFNC research in PTSD[29–32] by demonstrating that brain network states can not only correlate with current symptom severity but also link with future PTSD symptoms. This ability to predict future symptom severity is particularly beneficial as it may enable earlier intervention strategies and tailored treatment plans and potentially prevent the progression of the disorder[43,44]. Moreover, the significant sex-specific differences in connectivity patterns we observed have not been detailed to this extent in earlier dFNC studies, providing new insights into how sex may influence the link between dFNC variables and the pathophysiology of PTSD.

In our study sample, comprising participants exposed to traumatic events, we analyzed dFNC and differentiated three distinct brain network states. Two of the three states (states 2 and 3) exhibited a higher degree of integration in the sensory network, while state 1 demonstrated a more disconnected sensory network. State 3 manifested the strongest connectivity within the CCN, within the CBN and between the CBN and the SCN. Moreover, we found that state 1 was characterized by intra-network connectivity, while the other two states exhibited inter-network connections with both strong negative and positive connectivity among brain networks. These observations collectively highlight that brain networks display substantial dynamism, a characteristic they maintain even without the presence of external stimuli as has been observed in other brain disorders[21–25,29,40]. In addition, we investigated whether the dynamics of brain networks in participants with PTS differed from those in the non-PTS group. Upon separately analyzing data from both groups of participants, we observed that each

group generated similar dFNC states, as expected and observed in other disorders[45]. This suggests that the dynamic nature of brain networks persists irrespective of PTS, highlighting the potential complexities and resilience of the brain's network dynamics in the face of trauma and related disorders.

A previous study, employing the same population as the current research, demonstrated that the static functional connectivity between the left dorsolateral prefrontal cortex and the arousal network, as well as between the right inferior temporal gyrus and the DMN, could predict both WK2 and M3 PCL-5 scores[20]. In the current study, we found that the whole-brain OCRs estimated from dFNC link with the PCL-5 at the time of neuroimaging data collection (WK2), as well as the PCL-5 scores 10 weeks post-data collection (M3). Our new analyses contribute to a deeper understanding of the neurobiological mechanisms underlying PTSD by looking at brain network dynamics.

Specifically, we found that participants with higher PCL-5 scores tend to spend more time in an intra-network brain state, referred to as state 1. Importantly, the amount of time spent in this state was found to link with future symptom severity at M3 (Fig. 3a). Supplementary Fig. 4 provides additional insights into the relationship between the OCR of state 1 and PTSD symptom severity. State 1 is characterized by reduced connectivity among sensory networks, including visual, auditory and sensory motor networks. Furthermore, our results confirmed that spending more time in an inter-network brain state (state 3) is negatively correlated with PCL-5 scores at WK2 and M3 (Fig. 3a). State 3 is characterized by increased connectivity among sensory networks, suggesting enhanced information exchange and integration between these networks. Previous studies have consistently reported alterations in visual processing, as well as auditory processing, in individuals with PTSD[46,47]. Multiple neuroimaging studies have demonstrated alterations in the functioning of the visual, auditory and motor cortices among participants with PTSD[47–49]. Notably, abnormal activation in the visual cortex during picture-viewing tasks has been observed in these individuals[47]. Furthermore, significant alterations in visual processing have been identified within the ventral visual stream, which is responsible for processing object properties[47]. This suggests that PTSD may affect the specific components of the visual system involved in object recognition and perception, as previous findings, including those from the AURORA study, highlight a role for structural integrity of the ventral visual stream in the development of PTSD[50,51]. Our current findings, in conjunction with previous reports of subtle deficits in sensory networks, particularly the visual sensory system in PTSD, provide compelling evidence that disruptions in information integration among sensory networks are closely linked to the severity of PTSD symptoms[50–53]. Enhancing the connectivity and integration within these networks could potentially serve as a therapeutic target for mitigating symptom severity and improving outcomes in individuals with PTSD[54].

In addition to the sensory networks, our findings reveal that state 1 is characterized by relatively lower within-CBN connectivity and between-CBN-and-SCN connectivity (that is, CBN/SCN) compared with the other two states. This observation aligns with previous structural neuroimaging studies that have reported reduced cerebellar volumes in individuals with PTSD[55,56]. Furthermore, functional neuroimaging studies have provided corresponding evidence by demonstrating alterations in neural activity and functional connectivity of the cerebellum in PTSD[57]. Our new finding, that participants with higher PCL-5 scores spent more time in the state characterized by lower CBN connectivity, adds another layer of information to the understanding of temporal network patterns associated with CBN in PTSD. This suggests that alterations in cerebellar connectivity patterns may play a role in modulating symptom severity and could serve as potential markers for the disorder.

In the subsequent analysis, we investigated the influence of sex on the relationship between brain network dynamics and symptom severity. We observed that the association between OCRs and PCL-5 scores was more prominent in the female group. Specifically, the correlation between state 1 OCR and WK2 PCL-5 as well as the correlation between state 3 OCR and WK2 PCL-5 was statistically significant within the female group, and the strength of this correlation was notably higher in the female group compared with the male group (Fig. 3b,c).

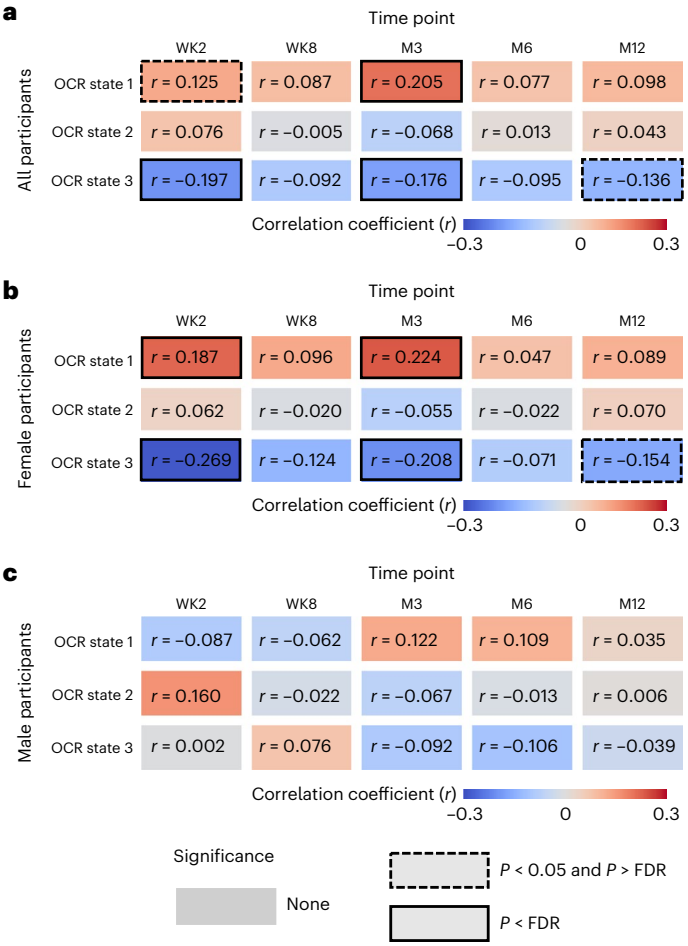

Fig. 3 | dFNC OCRs link with PCL-5. We employed a GLM to explore the association between OCRs and PCL-5 scores using data from all participants at WK2 (N = 275), WK8 (N = 243), M3 (N = 226), M6 (N = 208) and M12 (N = 176). We included age, sex at birth, years of education, income, employment status, marital status, scanning site, type of trauma and percentile ADI as covariates. In the sex-stratified analysis, sex was excluded as a covariate. With 3 predictors and 5 time points, we have 15 tests. These data were analyzed using a two-sided test to assess the significance of associations in both directions. In each panel, all 15 P values have been adjusted for multiple comparisons using FDR correction. **a**, We found a positive association between the OCR of state 1 and PCL-5 scores at M3 (r = 0.205, β = 0.0042, SE = 0.0012, 95% CI: 0.0018–0.0066, $P_{corrected}$ = 0.0079, N = 226). We also found a significant negative association between the OCR of state 3 and PCL-5 scores of WK2 (r = -0.197, β = -0.0033, SE = 0.0009, 95% CI: −−0.0052 to −0.0013, $P_{corrected}$ = 0.0079, N = 275) and between state 3 OCR and PCL-5 scores at M3 (r = -0.176, β = -0.0032, SE = 0.0011, 95% CI: −−0.0054 to −0.0011, $P_{corrected}$ = 0.0176, N = 226). **b**, A positive association is observed between the OCR of state 1 and PCL-5 scores both WK2 (r = 0.187, β = 0.0034, SE = 0.0014, 95% CI: -0.0001–0.0045, $P_{corrected}$ = 0.044, N = 181) and M3 (r = 0.224, β = 0.0044, SE = 0.0014, 95% CI: 0.00180–0.0066, $P_{corrected}$ = 0.019, N = 154). Conversely, a negative correlation is seen between the OCR of state 3 and PCL-5 scores at both WK2 (r = -0.269, β = -0.0043, SE = 0.0011, 95% CI: −−0.0052 to −0.0013, $P_{corrected}$ = 0.004, N = 181) and M3 (r = -0.208, β = −0.0036, SE = 0.0013, 95% CI: −−0.0055 to −0.0011, $P_{corrected}$ = 0.014, N = 154). **c**, We did not find any significant result for the male group. The color bar represents correlation strength, with solid box outlines indicating significant results after FDR correction and dashed box outlines marking significant results that did not survive correction.

https://doi.org/10.1038/s44220-024-00377-0

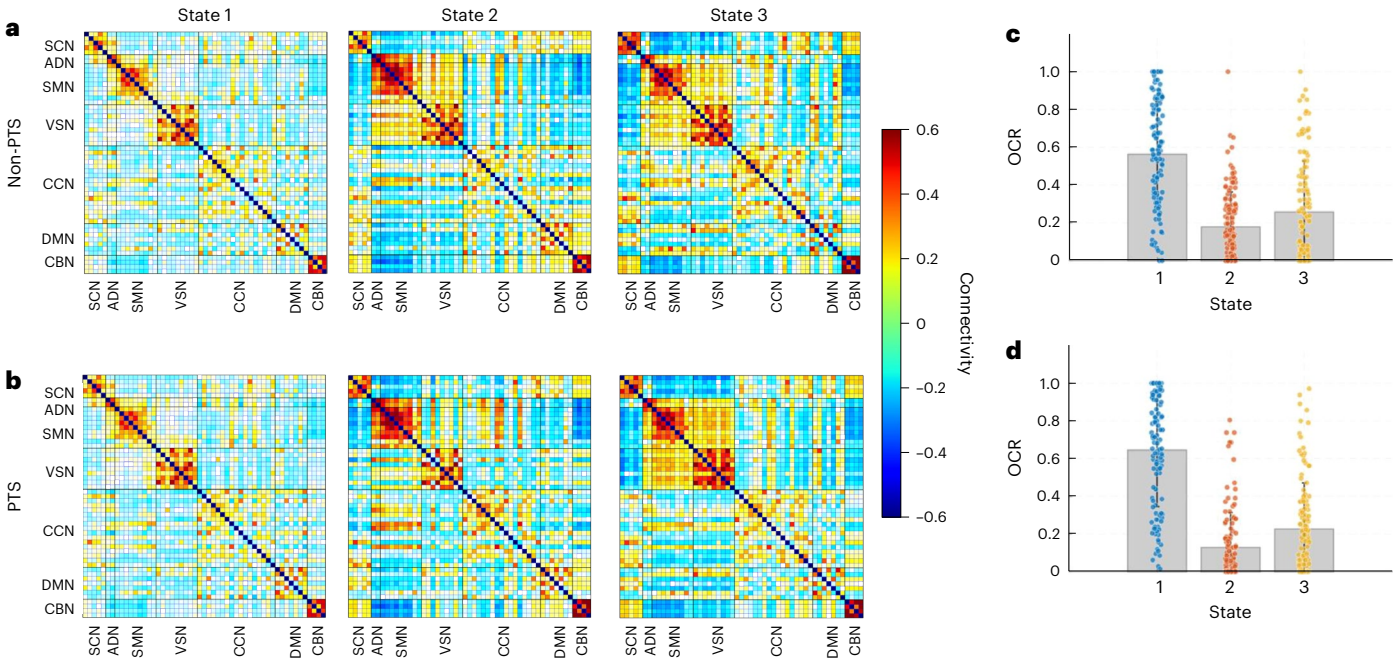

Fig. 4 | Both non-PTS and PTS groups generate similar dFNC state. a, The dFNC states identified only in the non-PTS group ($N = 151$). **b**, The dFNC states identified only in the PTS group ($N = 124$). **c**, The OCR in different states of the non-PTS group ($N = 151$). **d**, The OCR in different state of the PTS group ($N = 124$). The bar plot shows the mean of OCR, and the error bar shows ±s.d. from the mean. The color bar indicates the strength of the connectivity.

Note that previous studies have extensively explored the role of sex in the development of PTSD, with emerging evidence suggesting differences in symptomatology and underlying neurobiology between male and female groups[33,58]. In line with these findings, our results further support the notion that the identified dFNC biomarkers, particularly when correlating with symptom severity, are stronger in female participants; this could potentially reflect the higher prevalence of PTS/PTSD in this demographic.

Recent large-scale genomic studies show that women of European and African ancestry may have higher heritability for PTSD than men, suggesting that genetic factors may also play a significant role in the disorder's development, particularly in interaction with sex differences[59,60]. However, it is important to note that biological sex is not the primary determinant of the various neurophenotypes associated with adverse post-traumatic outcomes; other factors such as low socioeconomic status also play a significant role[34,35]. To avoid a narrow focus on sex alone, our analysis considered all available socioeconomic and demographic factors from the dataset. This approach allowed us to conduct a comprehensive analysis of the connection between OCRs and PTSD symptom severity, specifically considering the sex effect. In addition, women's risk for PTSD is partially determined by the fact that they experience sexual traumas more frequently. For example, a study shows that women exhibit almost twice the PTSD symptoms in sexual assault survivors[61]. However, in the AURORA dataset, the type of trauma does not play a major role in driving sex differences. The traumas are primarily motor vehicle collisions for both women and men, yet sex differences in dFNC link with PTSD symptom severity are still observed.

Our findings highlight the potential of inter-network connectivity as a protective mechanism against PTSD. Specifically, our results suggest that transitioning the brain from a risk state (state 1) to a protective state (state 3) could be therapeutically beneficial. This insight is particularly applicable to closed-loop therapies such as closed-loop neuromodulation[62] and neurofeedback[63,64], which can be tailored to induce such state transitions. State-dependent brain stimulation, which adjusts its parameters on the basis of the current brain state, offers a promising approach to dynamically target and ameliorate high-risk states effectively[65–67]. Administering neuromodulation when the brain is in a high-risk state and transitioning it to a more protective state could enhance therapeutic outcomes by leveraging the brain's natural functional network dynamics[68]. While the implementation of real-time, state-specific interventions presents technical challenges, including the real-time analysis of brain states and concurrent neuromodulation[69], the potential to mitigate PTSD symptoms preemptively could transform early intervention strategies.

Several limitations should be acknowledged while interpreting the present findings. The overall sample size was relatively modest, and the sample sizes among the comparison groups (male group versus female group) were not the same. Furthermore, participants who completed all scans and had more complete datasets may differ from those who did not complete all scans, making it unclear whether the results apply to dropouts who may be at higher risk for PTSD after trauma. In this study, we examined dFNC in individuals with PTS and a non-PTS group, both of whom were exposed to trauma. To gain a comprehensive understanding, further research is required to directly compare the dFNC variables among the PTSD group, a group of healthy individuals exposed to a traumatic event and a group of healthy individuals who have not undergone any traumatic experiences. However, we assume that healthy individuals exposed to trauma could serve as a more suitable control group for those with PTSD, facilitating our understanding of the underlying neural processes of PTSD. Due to the data-driven approach employed in our study, which utilizes group independent component analysis[70] to identify independent components, we do not have direct measurements of amygdala dynamics. However, we have identified one of the 53 components as a proxy for amygdala activity. Supplementary Fig. 5 provides more details about the dynamics of the amygdala in our study population, as analyzed in our pipeline. In addition, in this study, we investigated the relationship between dFNC variables and the severity of PTSD symptoms at various time points. However, to enhance our understanding, future research should compare dFNC variables among groups exhibiting different PTSD trajectories during a one-year assessment. In our study, we utilized the initial neuroimaging data available from the AURORA study, which was collected 2 weeks post-trauma, before any PTSD diagnosis at week 8.

Given that the AURORA study also gathered neuroimaging data at 6 months post-trauma, future research would benefit from examining the dFNC patterns using the resting-state fMRI data from this later time point. Such analysis could yield more profound insights into the evolving brain dynamics associated with PTSD. Finally, we observed low correlation values between dFNC variables and PTSD symptom severity, ranging from −0.269 to +0.224. This modest correlation may be influenced by several factors: the limited informativeness of the dFNC variables compared with other brain variables such as structural—a finding similarly reported in the previous AURORA study, albeit with different brain variables[58,71]. In addition, the relatively small sample size in our study might contribute to the low correlation values. However, previous PTSD studies with larger sample sizes have also reported low correlations between brain variables and symptom severity[72]. Minimal variance in brain variables among trauma-exposed individuals may further contribute to these results.

Conclusions

In summary, our investigation into the dFNC of civilians recently exposed to trauma revealed distinct patterns in brain network dynamics. Our findings indicate that the duration participants spent in certain brain network states can link with both their current and subsequent PCL-5 scores. Specifically, we identified that spending time in an intra-network brain state is associated with higher PCL-5 scores, while engagement in an inter-network brain state correlates with lower PCL-5 scores. Furthermore, our analysis highlighted the role of multiple brain networks encompassing the visual, auditory, sensory motor and cerebellar networks in PTSD. We also observed a stronger association between brain dynamics and PCL-5 scores in the female group compared with the male group. By incorporating sex-specific disparities, tailoring interventions and treatment strategies accordingly, we can potentially develop more effective and personalized approaches for PTSD.

Methods

Inclusion and ethics statement

The study was conducted in accordance with ethical guidelines and received approval from the institutional review board (IRB) at the University of North Carolina (IRB no. 1707-03) on 12 May 2017, covering multiple sites. Additional sites either entered into reliance agreements or conducted parallel IRB reviews. Participants provided written informed consent before participation. An independent medical monitor evaluated and approved the procedures for handling any cases of clinical deterioration reported by participants or identified by study staff. This monitor also reviewed detailed reports of participant interactions prepared by experienced clinicians.

Study population

Participants were recruited as part of the multisite ED AURORA study[38]. The study targeted individuals who had experienced a traumatic event necessitating an ED evaluation, with recruitment occurring within 72 h of the event[38]. This cohort of early post-trauma participants was selected to explore pivotal changes in neurobiology and brain function that could heighten the risk for trauma-related psychopathology in the subsequent weeks or months. The study aimed to enroll a demographically representative sample of the US population without restrictions on demographic variables such as sex, gender, race or ethnicity.

In this study, the participants who experienced incidents such as a car accident, a high fall (>10 feet), a physical assault, sexual violence or mass casualty incident were considered to have experienced trauma. The inclusion criteria included (1) aged between 18 and 75 years, (2) being alert and oriented at the ED, (3) having the ability to speak and write English fluently, (4) having no cognitive impairment and (5) having the ability to use the smartphone for >1 year post-enrollment. Exclusion criteria included solid organ damage, severe bleeding, a requirement for a chest tube and the likelihood of being admitted for longer than 72 h. The study eventually included 2,943 AURORA participants with clinical item-level data, recruited between September 2017 and June 2021, marking the final data freeze for psychometric release (Freeze 4.0 dataset at 22 September 2021). Participants recruited at one of the ED locations for the AURORA study, which directed participants to one of five 'deep phenotyping' sites, were invited to undergo MRI scans. These scans were conducted either in the morning or in the afternoon, approximately 2 weeks following the traumatic event (WK2). After thorough preprocessing and quality checks, data from 275 participants were included in our study (Supplementary Fig. 6).

Race and ethnicity

The race/ethnicity parameter reflects the participant's background based on self-reported data collected during the initial ED baseline survey. This variable is an integer ranging from 1 to 4, categorizing ethnic backgrounds as 1 for Hispanic, 2 for non-Hispanic white, 3 for non-Hispanic Black and 4 for non-Hispanic other. Classification is determined from responses to two survey questions—one about Hispanic, Latino or Spanish origin and another concerning race. An algorithm uses these self-reported responses to assign participants to one of these groups, or marks the data as missing if responses are incomplete.

Clinical measures

The PCL-5 was administered to assess PTSD symptoms at multiple time points, including WK2, WK8, M3, M6 and M12, as depicted in Fig. 1a. It is important to emphasize that different time frames were considered for each of the time points: the WK2 assessment reflected symptoms experienced over the past two weeks, while assessments from WK8 onward considered symptoms over the past 30 days. This longitudinal assessment allows for a comprehensive understanding of the participants' PTSD symptomatology throughout the study duration. Table 1 summarizes the demographic and clinical characteristics of the participants included in this study. In addition, to distinguish individuals with PTS from those without PTS in WK2 of the study, we employ a threshold for the PCL-5 at 31. Participants with a PCL-5 score greater than 31 are classified as having PTS, while those with a score less than 31 are considered non-PTS[39]. It is important to note that we refer to this group as having PTS and not PTSD, as the PTSD diagnosis was made in W8, while we used the WK2 PCL-5 scores to identify these two groups. Supplementary Fig. 1 illustrates the distribution of PCL-5 scores for individuals included in this study at various time points. In addition, a detailed comparison of clinical and psychological metrics across sex in the non-PTS and PTS groups is presented in Supplementary Table 1. Supplementary Fig. 7 displays the number of PTSD and non-PTSD participants diagnosed with PTSD during subsequent assessments at WK8 and at M3, M6 and M12 after the traumatic event.

Types of traumatic events in the AURORA study

The AURORA study meticulously classifies traumatic events into specific categories to facilitate detailed analysis and understanding. Motor vehicle collisions may involve participants inside, on top of or struck by various motorized vehicles such motorcycles and ATVs. Non-motorized collisions include incidents involving bicycles and skateboards. Physical assault encompasses intentional injuries inflicted by another person, while sexual assault covers any sexual contact, ranging from groping to rape. Falls are categorized by height, with distinctions made between falls from above and below 10 feet, noting that a fall from 10 feet is typically equivalent to falling from a one-story building. Incidents causing traumatic-stress exposure to many people refer to large-scale disasters that affect the participant along with others, such as plane crashes or natural disasters. Poisoning includes the ingestion or inhalation of toxic substances; burns cover injuries from thermal, electrical, chemical sources, radiation or friction; and animal-related traumas involve reactions to stings or bites. This structured classification aids in the tailored analysis and support for those affected by various types of traumatic experiences.

Imaging acquisition protocol

Participants underwent a thorough screening process before undergoing scanning, which involved checking for any contraindications to MRI or other exclusion criteria. For female participants and those who could potentially be pregnant, a pregnancy test was administered before entering the MRI environment. MRI scans were conducted using 3T Siemens scanners at each site. While the scan sequences remained largely consistent across imaging sites, some variations in sequence parameters were present due to differences in hardware. The imaging protocol for each site is outlined in Supplementary Table 2. The resting-state imaging procedure lasted approximately 9 min, during which participants were instructed to keep their eyes open. They were asked to focus on the white cross displayed at the center of the screen and maintain a state of stillness throughout the imaging session[20].

Preprocessing

We corrected the differences in image acquisition times between slices using the statistical parametric mapping[73] default slice timing routines. The slice acquired in the middle of the sequence was chosen as the reference slice. The participant's head movement was then corrected using a rigid body, and three-dimensional brain translations and three-dimensional rotations were estimated. Next, the imaging data were resampled to $3 \times 3 \times 3$ mm^3 and spatially normalized to the Montreal Neurological Institute space using the echo-planar imaging template and the group ICA in the Neuromark template toolbox's default bounding box. The fMRI images were then smoothed using a Gaussian kernel with a full width at half maximum of 6 mm. We emphasize that while participants in this study have also been featured in other AURORA analyses and resting-state studies[20,74], the current analyses are distinct. In addition, the preprocessing approach diverges from the standard protocols commonly employed in AURORA research to align with methodologies used in our other work. A similar preprocessing approach has been employed in several of our previous studies[23–25,45,75].

Extracting independent components using Neuromark

We applied a hybrid Neuromark framework to extract the meaningful networks for each participant. The Neuromark framework is based on the Neuromark template derived from two large datasets, including the human connectome project (823 participants after the participant selection) and genomics superstruct project (1,005 participants after the participant selection). This framework has been successfully implemented in many studies with a wide range of brain imaging markers identified across different brain diseases[23–25,45,75]. Details of the construction of the templates can be found in our previous Neuromark paper[76].

The Neuromark template consists of 53 independent components (ICs), which were grouped into seven functional networks on the basis of anatomic and functional prior knowledge. These networks are subcortical network (SCN), auditory network (ADN), sensorimotor network (SMN), visual network (VSN), cognitive control network (CCN), default mode network (DMN) and cerebellar network (CBN) (Fig. 1b)[45]. All 53 ICs and their coordination are shown in Supplementary Table 3. We used these priors (the Neuromark_fMRI_1.0 template, available in GIFT (http://trendscenter.org/software/gift) and on the TReNDS website (http://trendscenter.org/data)) to run a fully automated independent component analysis in GIFT v.4.0.5.14 (ref. 70). We further (1) detrended linear, quadratic and cubic trends; (2) conducted multiple regression on the six realignment parameters and their temporal derivatives; (3) despiked detected outliers; and (4) applied a low-pass filter (cut-off frequency at 0.15 Hz) to remove noise and artifacts.

Dynamic FNC estimation

The dFNC of the whole brain was estimated via a sliding window approach, as shown in Fig. 2c (Step 1). We used a tapered window obtained by convolving a rectangle (window size = 20 TR = 47.2 s) with a Gaussian ($\sigma = 3$) to localize the dataset at each time point. Previous research revealed that a window size between 30 and 60 s is a suitable option for capturing dFNC variation[77]. Thus we assumed that a window size of 47.2 s is a reasonable choice. Next, within each window, we employed Pearson correlation to assess the FNC among all 53 ICs within each window. Given the 53 ICs, this resulted in a symmetric 53×53 matrix. Furthermore, with these 53 ICs, we derived a total of $\binom{53}{2} = 1,378$ connectivity variables for each window, encapsulating the comprehensive interconnections among the components. We then concatenated the dFNCs of each participant to form a $(C \times C \times T)$ array (where $C = 53$ denotes the number of ICs and $T = 210$), which represents the changes in brain connectivity between ICs as a function of time[45].

Dynamic FNC clustering

We next concatenated the dFNC of all participants and applied the k-means clustering algorithm to the dFNC windows to partition the data into sets of distinct clusters representing transient connectivity 'states' (as shown in Step 2 of Fig. 1c)[23–25,75]. The optimal number of cluster order was estimated using the elbow criterion based on the ratio of within- to between-cluster distances. By sweeping the k value from 2 to 9, we found that the optimal number of clusters was three[24]. We used Euclidian distance as a distance metric in this k-means clustering algorithm with 1,000 iterations. The k-means clustering analysis yielded three distinct states across all 275 participants and a state vector for each individual. The state vector reflects the temporal changes in whole-brain FNC. Subsequently, we determined the OCR for each participant, which is the proportion of time spent in each state. To compute the OCR for state i for a participant, we counted the number of windows in state i attributed to that participant and divided this by 210 (the total number of windows). Thus we obtained three OCR values for each individual, corresponding to the three states. (Step 3 in Fig. 1c). Two representative state vectors of PTS and non-PTS individuals and their associated OCR for each state are shown in Supplementary Fig. 3.

Statistical analysis

We employed a GLM to explore the association between OCRs and PCL-5 scores using data from all participants ($N = 275$). Our analysis included covariates such as age, sex at birth, years of education, income, employment status, marital status, scanning site, type of trauma and percentile ADI. We constructed individual models for each OCR and time point, resulting in a total of 15 models derived from the combination of 3 predictors and 5 time points. In addition, we developed 15 models for the male group ($N = 94$) and the female group ($N = 181$). In the context of sex-stratified analyses, sex itself was excluded as a covariate, and the analysis was run separately for each sex group. Therefore, we had 15 models for the whole-group analysis, 15 models for the female-group analysis and 15 models for the male-group analysis. A Benjamini–Hochberg FDR correction was applied to account for the 15 significance tests corresponding to the correlations of each analysis[78]. In this study, all data analysis and statistical computations were conducted using MATLAB software (MathWorks) version R2022b.

Reporting summary

Further information on research design is available in the Nature Portfolio Reporting Summary linked to this article.

Data availability

The data utilized in the preparation of this manuscript are publicly available in the National Institute of Mental Health (NIMH) Data Archive (NDA). The dataset identifier for this study is NIMH Data Archive Digital Object Identifier https://doi.org/10.15154/zwyn-rb26.

Code availability

The code used for preprocessing and dFNC calculation is available at https://trendscenter.org/software/. Statistical parametric mapping (SPM 12) is available at https://www.fil.ion.ucl.ac.uk/spm/.

The Neuromark framework and the Neuromark template (Neuromark_fMRI_1.0) have been made available and incorporated into the Group ICA Toolbox (GIFT v.4.0.5.14: https://trendscenter.org/software/gift/). Users worldwide can now directly download and utilize these resources. The chord graphs are generated using the NiChord toolbox in Python (https://github.com/paulcbogdan/NiChord). The general linear model (GLM) code in MATLAB is available at https://www.mathworks.com/help/stats/fitglm.html.

References

1. Pitman, R. K. et al. Biological studies of post-traumatic stress disorder. *Nat. Rev. Neurosci.* **13**, 769–787 (2012).
2. Pacella, M. L., Hruska, B. & Delahanty, D. L. The physical health consequences of PTSD and PTSD symptoms: a meta-analytic review. *J. Anxiety Disord.* **27**, 33–46 (2013).
3. Schmidt, U., Kaltwasser, S. F. & Wotjak, C. T. Biomarkers in posttraumatic stress disorder: overview and implications for future research. *Dis. Markers* **35**, 43–54 (2013).
4. Michopoulos, V., Norrholm, S. D. & Jovanovic, T. Diagnostic biomarkers for posttraumatic stress disorder: promising horizons from translational neuroscience research. *Biol, Psychiatry* **78**, 344–353 (2015).
5. Al Jowf, G. I., Ahmed, Z. T., Reijnders, R. A., de Nijs, L. & Eijssen, L. M. T. To predict, prevent, and manage post-traumatic stress disorder (PTSD): a review of pathophysiology, treatment, and biomarkers. *Int. J. Mol. Sci.* **24**, 5238 (2023).
6. Roeckner, A. R., Oliver, K. I., Lebois, L. A. M., van Rooij, S. J. H. & Stevens, J. S. Neural contributors to trauma resilience: a review of longitudinal neuroimaging studies. *Transl. Psychiatry* **11**, 508 (2021).
7. Neria, Y. Functional neuroimaging in PTSD: from discovery of underlying mechanisms to addressing diagnostic heterogeneity. *Am. J. Psychiatry* **178**, 128–135 (2021).
8. Carrion, V. G., Wong, S. S. & Kletter, H. Update on neuroimaging and cognitive functioning in maltreatment-related pediatric PTSD: treatment implications. *J. Fam. Violence* **28**, 53–61 (2013).
9. Chen, H. J. et al. Altered resting-state dorsal anterior cingulate cortex functional connectivity in patients with post-traumatic stress disorder. *Aust. N. Z. J. Psychiatry* **53**, 68–79 (2019).
10. Shaw, M. E. et al. Abnormal functional connectivity in posttraumatic stress disorder. *Neuroimage* **15**, 661–674 (2002).
11. Jin, C. et al. Abnormalities in whole-brain functional connectivity observed in treatment-naive post-traumatic stress disorder patients following an earthquake. *Psychol. Med.* **44**, 1927–1936 (2014).
12. van Rooij, S. J. H. et al. The role of the hippocampus in predicting future posttraumatic stress disorder symptoms in recently traumatized civilians. *Biol. Psychiatry* **84**, 106–115 (2018).
13. Stevens, J. S. et al. Disrupted amygdala–prefrontal functional connectivity in civilian women with posttraumatic stress disorder. *J. Psychiatr. Res.* **47**, 1469–1478 (2013).
14. Breukelaar, I. A., Bryant, R. A. & Korgaonkar, M. S. The functional connectome in posttraumatic stress disorder. *Neurobiol. Stress* **14**, 100321 (2021).
15. Lebois, L. A. M. et al. Large-scale functional brain network architecture changes associated with trauma-related dissociation. *Am. J. Psychiatry* **178**, 165–173 (2021).
16. Garrett, A. et al. Longitudinal changes in brain function associated with symptom improvement in youth with PTSD. *J. Psychiatr. Res.* **114**, 161–169 (2019).
17. Malivoire, B. L., Girard, T. A., Patel, R. & Monson, C. M. Functional connectivity of hippocampal subregions in PTSD: relations with symptoms. *BMC Psychiatry* **18**, 129 (2018).
18. Suo, X. et al. Individualized prediction of PTSD symptom severity in trauma survivors from whole-brain resting-state functional connectivity. *Front. Behav. Neurosci.* **14**, 563152 (2020).
19. Belleau, E. L. et al. Amygdala functional connectivity in the acute aftermath of trauma prospectively predicts severity of posttraumatic stress symptoms: functional connectivity predicts future PTSD symptoms. *Neurobiol. Stress* **12**, 100217 (2020).
20. Harnett, N. G. et al. Prognostic neuroimaging biomarkers of trauma-related psychopathology: resting-state fMRI shortly after trauma predicts future PTSD and depression symptoms in the AURORA study. *Neuropsychopharmacology* **46**, 1263–1271 (2021).
21. Schumacher, J. et al. Dynamic functional connectivity changes in dementia with Lewy bodies and Alzheimer's disease. *Neuroimage Clin.* **22**, 101812 (2019).
22. Rabany, L. et al. Dynamic functional connectivity in schizophrenia and autism spectrum disorder: convergence, divergence and classification. *Neuroimage Clin.* **24**, 101966 (2019).
23. Sendi, M. S. E. et al. Aberrant dynamic functional connectivity of default mode network in schizophrenia and links to symptom severity. *Front. Neural Circuits* **15**, 649417 (2021).
24. Dini, H. et al. Dynamic functional connectivity predicts treatment response to electroconvulsive therapy in major depressive disorder. *Front. Hum. Neurosci.* **15**, 689488 (2021).
25. Sendi, M. S. E. et al. Aberrant dynamic functional connectivity of default mode network predicts symptom severity in major depressive disorder. *Brain Connect.* https://doi.org/10.1089/brain.2020.0748 (2021).
26. Allen, E. A. et al. Tracking whole-brain connectivity dynamics in the resting state. *Cereb. Cortex* **24**, 663–676 (2014).
27. Preti, M. G., Bolton, T. A. & Van De Ville, D. The dynamic functional connectome: state-of-the-art and perspectives. *Neuroimage* **160**, 41–54 (2017).
28. Calhoun, V. D., Miller, R., Pearlson, G. & Adali, T. The chronnectome: time-varying connectivity networks as the next frontier in fMRI data discovery. *Neuron* **84**, 262–274 (2014).
29. Fu, Z. et al. Dynamic functional network connectivity associated with post-traumatic stress symptoms in COVID-19 survivors. *Neurobiol. Stress* **15**, 100377 (2021).
30. Dai, Y. et al. Altered dynamic functional connectivity associates with post-traumatic stress disorder. *Brain Imaging Behav.* https://doi.org/10.1007/s11682-023-00760-y (2023).
31. Wen, Z., Seo, J., Pace-Schott, E. F. & Milad, M. R. Abnormal dynamic functional connectivity during fear extinction learning in PTSD and anxiety disorders. *Mol. Psychiatry* **27**, 2216–2224 (2022).
32. Fu, S. et al. Altered local and large-scale dynamic functional connectivity variability in posttraumatic stress disorder: a resting-state fMRI study. *Front. Psychiatry* **10**, 234 (2019).
33. Dobie, D. J. et al. Posttraumatic stress disorder in female veterans association with self-reported health problems and functional impairment. *Arch. Intern. Med.* **164**, 394–400 (2004).
34. Golin, C. E. et al. Post-traumatic stress disorder symptoms and mental health over time among low-income women at increased risk of HIV in the US. *J. Health Care Poor Underserved* **27**, 891–910 (2016).
35. Rees, S. J. et al. A high-risk group of pregnant women with elevated levels of conflict-related trauma, intimate partner violence, symptoms of depression and other forms of mental distress in post-conflict Timor–Leste. *Transl. Psychiatry* **6**, e725 (2016).
36. Rayburn, N. R. et al. Trauma, depression, coping, and mental health service seeking among impoverished women. *J. Consult. Clin. Psychol.* **73**, 667–677 (2005).
37. Webb, E. K. et al. Neural impact of neighborhood socioeconomic disadvantage in traumatically injured adults. *Neurobiol. Stress* **15**, 100385 (2021).
38. McLean, S. A. et al. The AURORA study: a longitudinal, multimodal library of brain biology and function after traumatic stress exposure. *Mol. Psychiatry* **25**, 283–296 (2020).

39. Bovin, M. J. et al. Psychometric properties of the PTSD checklist for diagnostic and statistical manual of mental disorders-fifth edition (PCL-5) in veterans. *Psychol. Assess.* **28**, 1379–1391 (2016).
40. Du, Y., Fu, Z. & Calhoun, V. D. Classification and prediction of brain disorders using functional connectivity: promising but challenging. *Front. Neurosci.* https://doi.org/10.3389/fnins.2018.00525 (2018).
41. Jin, C. et al. Dynamic brain connectivity is a better predictor of PTSD than static connectivity. *Hum. Brain. Mapp.* **38**, 4479–4496 (2017).
42. Tozlu, C., Jamison, K., Gauthier, S. A. & Kuceyeski, A. Dynamic functional connectivity better predicts disability than structural and static functional connectivity in people with multiple sclerosis. *Front. Neurosci.* **15**, 763966 (2021).
43. Tejavibulya, L. et al. Predicting the future of neuroimaging predictive models in mental health. *Mol. Psychiatry* **27**, 3129–3137 (2022).
44. Bertocci, M. A. et al. Altered patterns of central executive, default mode and salience network activity and connectivity are associated with current and future depression risk in two independent young adult samples. *Mol. Psychiatry* **28**, 1046–1056 (2023).
45. Sendi, M. S. E. et al. Alzheimer's disease projection from normal to mild dementia reflected in functional network connectivity: a longitudinal study. *Front. Neural Circuits* **14**, 593263 (2021).
46. MacGregor, A. J., Joseph, A. R., Walker, G. J. & Dougherty, A. L. Co-occurrence of hearing loss and posttraumatic stress disorder among injured military personnel: a retrospective study. *BMC Public Health* **20**, 1076 (2020).
47. Mueller-Pfeiffer, C. et al. Atypical visual processing in posttraumatic stress disorder. *Neuroimage Clin.* **3**, 531–538 (2013).
48. Rangaprakash, D., Dretsch, M. N., Katz, J. S., Denney, T. S. & Deshpande, G. Dynamics of segregation and integration in directional brain networks: illustration in soldiers with PTSD and neurotrauma. *Front. Neurosci.* **13**, 803 (2019).
49. Lobo, I. et al. Hidden wounds of violence: abnormal motor oscillatory brain activity is related to posttraumatic stress symptoms. *Neuroimage* **224**, 117404 (2021).
50. Harnett, N. G. et al. Structural covariance of the ventral visual stream predicts posttraumatic intrusion and nightmare symptoms: a multivariate data fusion analysis. *Transl. Psychiatry* **12**, 321 (2022).
51. Harnett, N. G. et al. Acute posttraumatic symptoms are associated with multimodal neuroimaging structural covariance patterns: a possible role for the neural substrates of visual processing in posttraumatic stress disorder. *Biol. Psychiatry Cogn. Neurosci. Neuroimaging* **7**, 129–138 (2022).
52. Zhang, Y. et al. Intranetwork and internetwork functional connectivity alterations in post-traumatic stress disorder. *J. Affect. Disord.* **187**, 114–121 (2015).
53. Shang, J. et al. Alterations in low-level perceptual networks related to clinical severity in PTSD after an earthquake: a resting-state fMRI study. *PLoS ONE* **9**, e96834 (2014).
54. Avrahami, D. Visual art therapy's unique contribution in the treatment of post-traumatic stress disorders. *J. Trauma Dissociation* **6**, 5–38 (2005).
55. Blithikioti, C. et al. The cerebellum and psychological trauma: a systematic review of neuroimaging studies. *Neurobiol. Stress* **17**, 100429 (2022).
56. Baldaçara, L. et al. Reduced cerebellar left hemisphere and vermal volume in adults with PTSD from a community sample. *J. Psychiatr. Res.* **45**, 1627–1633 (2011).
57. Lebois, L. A. M. et al. Persistent dissociation and its neural correlates in predicting outcomes after trauma exposure. *Am. J. Psychiatry* **179**, 661–672 (2022).
58. Borst, B. et al. Sex differences in response inhibition-related neural predictors of posttraumatic stress disorder in civilians with recent trauma. *Biol. Psychiatry Cogn. Neurosci. Neuroimaging* https://doi.org/10.1016/j.bpsc.2024.03.002 (2024).
59. Duncan, L. E. et al. Largest GWAS of PTSD (*N*=20 070) yields genetic overlap with schizophrenia and sex differences in heritability. *Mol. Psychiatry* **23**, 666–673 (2018).
60. Nievergelt, C. M. et al. International meta-analysis of PTSD genome-wide association studies identifies sex- and ancestry-specific genetic risk loci. *Nat. Commun.* **10**, 4558 (2019).
61. Rowland, G. E. et al. Prior sexual trauma exposure impacts posttraumatic dysfunction and neural circuitry following a recent traumatic event in the AURORA study. *Biol. Psychiatry Glob. Open Sci.* **3**, 705–715 (2023).
62. Gill, J. L. et al. A pilot study of closed-loop neuromodulation for treatment-resistant post-traumatic stress disorder. *Nat. Commun.* **14**, 2997 (2023).
63. Zweerings, J. et al. Rt-fMRI neurofeedback-guided cognitive reappraisal training modulates amygdala responsivity in posttraumatic stress disorder. *Neuroimage Clin.* **28**, 102483 (2020).
64. Lieberman, J. M. et al. Posterior cingulate cortex targeted real-time fMRI neurofeedback recalibrates functional connectivity with the amygdala, posterior insula, and default-mode network in PTSD. *Brain Behav.* **13**, e2883 (2023).
65. Bradley, C., Nydam, A. S., Dux, P. E. & Mattingley, J. B. State-dependent effects of neural stimulation on brain function and cognition. *Nat. Rev. Neurosci.* **23**, 459–475 (2022).
66. Lee, S. H. & Dan, Y. Neuromodulation of brain states. *Neuron* **76**, 209–222 (2012).
67. Mccormick, D. A., Nestvogel, D. B. & He, B. J. Neuromodulation of Brain State and Behavior. *Annu. Rev. Neurosci.* **43**, 391–415 (2020).
68. Sack, A. T. et al. Target engagement and brain state dependence of transcranial magnetic stimulation: implications for clinical practice. *Biol. Psychiatry* **95**, 536–544 (2024).
69. Monti, R. P. et al. Real-time estimation of dynamic functional connectivity network. *Hum. Brain Mapp.* **38**, 202–220 (2017).
70. Calhoun, V. D., Liu, J. & Adali, T. A review of group ICA for fMRI data and ICA for joint inference of imaging, genetic, and ERP data. *Neuroimage* **45**, S163–S172 (2009).
71. van Rooij, S. J. H. et al. Defining the *r* factor for post-trauma resilience and its neural predictors. *Nat. Ment. Health* https://doi.org/10.1038/s44220-024-00242-0 (2024).
72. Dennis, E. L. et al. Altered white matter microstructural organization in posttraumatic stress disorder across 3047 adults: results from the PGC-ENIGMA PTSD consortium. *Mol. Psychiatry* **26**, 4315–4330 (2021).
73. Friston, K. J. Statistical parametric mapping. In *Functional Neuroimaging: Technical Foundations* (eds Thatcher, R. W. et al.) 79–93 (Academic Press, 1994).
74. Harnett, N. G. et al. Structural inequities contribute to racial/ethnic differences in neurophysiological tone, but not threat reactivity, after trauma exposure. *Mol. Psychiatry* https://doi.org/10.1038/s41380-023-01971-x (2023).
75. Sendi, M. S. E. et al. The link between static and dynamic brain functional network connectivity and genetic risk of Alzheimer's disease. *Neuroimage Clin.* **37**, 103363 (2023).
76. Du, Y. et al. NeuroMark: an automated and adaptive ICA based pipeline to identify reproducible fMRI markers of brain disorders. *Neuroimage Clin.* **28**, 102375 (2020).
77. Yaesoubi, M., Adalı, T. & Calhoun, V. D. A window-less approach for capturing time-varying connectivity in fMRI data reveals the presence of states with variable rates of change. *Hum. Brain Mapp.* **39**, 1626–1636 (2018).
78. Benjamini, Y. & Hochberg, Y. Controlling the false discovery rate: a practical and powerful approach to multiple testing. *R. Stat. Soc. B* **57**, 289–300 (1995).

Acknowledgments

The investigators express their gratitude to the trauma survivors participating in the AURORA study. Their time and effort during a challenging period of their lives enable our work to improve recovery outcomes for future trauma survivors. The AURORA project was supported by the National Institute of Mental Health (NIMH) under U01MH110925, the US Army MRMC, One Mind and the Mayday Fund. The following authors received financial support from the AURORA project: R.C.K., K.J.R., K.C.K., S.A.M., S.L.H., F.L.B., X.A., J.S.S., T.C.N., G.D.C., T.J., S.D.L., L.T.G., K.A.B., S.L.R., J.P.H., A.B.S., C.L., P.I.M.Jr, P.L.H., S.S., C.W.J., B.E.P., R.A.S., V.P.M., J.L.P., M.J.S., E.H., C.P., D. A. Pizzagalli, R.C.M., R.M.D., N.K.R., B.J.O., L.D.S., S.E.B., D. A. Peak, J.F.S., and S.E.H. In addition, this project received support from NIMH under T32MH125786 (M.S.E.S.), Phyllis and Jerome Lyle Rappaport Mental Health Research Scholars Award (M.S.E.S.), K01MH129828 (N.G.H.), K01MH121653 (S.J.H.v.R.), R01MH129495 (T.J.), R01MH122867 (T.J.), R01MH121617 (L.T.G.) and R01MH123610 (V.D.C.). The content is the sole responsibility of the authors and does not necessarily represent the official views of the funders. The funders had no role in study design, data collection and analysis, decision to publish or manuscript preparation. Verily Life Sciences and Mindstrong Health provided some of the hardware and software for study assessments, and The Many Brains Project contributed software for neurocognitive assessments. This paper reflects the authors' views and may not reflect the opinions or views of the NIH or the submitters of original data to the NIMH Data Archive (NDA).

Author contributions

M.S.E.S., R.C.K., K.C.K., S.A.M., J.S.S., N.T.G., S.J.H.v.R., V.D.C. and K.J.R. contributed to the conceptualization, including formulation or evolution of overarching research goals and aims, of the study. M.S.E.S., V.V., D. A. Pizzagalli, S.L.H., F.L.B., X.A., T.C.N., G.D.C., T.J., S.D.L., L.T.G., K.A.B., S.L.R., J.F.S., S.E.H., R.C.K., K.C.K., S.A.M., J.S.S., V.D.C. and K.J.R. contributed to the methodology of the study, including development or design of methodology and creation of models. M.S.E.S. and Z.F. contributed to software development, which included programming, designing computer programs, implementing computer code and supporting algorithms, and testing existing code components. M.S.E.S. contributed to the formal analysis and validation, including the application of statistical, mathematical, computational and other formal techniques to analyze and synthesize study data. M.S.E.S. was responsible for data visualization, including preparing, creating and presenting the published work, specifically focusing on visualization and data presentation. Z.F. contributed to neuroimaging preprocessing and variable extraction. M.S.E.S., N.G.H., V.V., D. A. Pizzagalli, N.P.D., V.D.C. and K.J.R. were responsible for writing the original draft, including preparation, creation and presentation of the published work, and writing initial draft. All authors contributed to the paper by reviewing and editing the original draft. S.L.H., F.L.B., T.J., J.P.H., A.B.S., C.L., P.I.M.Jr, P.L.H., S.S., C.W.J., B.E.P., N.T.G., V.P.M., L.A.H., R.A.S., J.L.P., M.J.S., E.H., A.M.C., C.P., D.A. Peak, R.C.M., R.M.D., N.K.R., B.J.O., P.S., L.D.S., S.E.B., J.S.S., S.A.M., R.C.K., K.C.K. and K.J.R. were responsible for project administration, including management and coordination, and were accountable for the planning and execution of the research activities. S.L.H., F.L.B., X.A., J.S.S., T.C.N., G.D.C., T.J., S.D.L., L.T.G., K.A.B., S.L.R., J.P.H., A.B.S., C.L., P.I.M.Jr, P.L.H., S.S., C.W.J., B.E.P., N.T.G., V.P.M., L.A.H., R.A.S., J.L.P., M.J.S., E.H., A.M.C., C.P., D.A. Peak, R.C.M., R.M.D., N.K.R., B.J.O., L.D.S., S.A.M., R.C.K., K.J.R. and K.C.K. conducted the research and investigation process, specifically, performing the experiments or data and evidence collection. S.L.H., F.L.B., X.A., J.S.S., T.C.N., G.D.C., T.J., S.D.L., L.T.G., K.A.B., S.L.R., J.P.H., A.B.S., C.L., P.I.M.Jr, P.L.H., S.S., C.W.J., B.E.P., N.T.G., V.P.M., L.A.H., R.A.S., J.L.P., M.J.S., E.H., A.M.C., C.P., D.A. Peak, R.C.M., R.M.D., N.K.R., B.J.O., P.S., S.E.B., L.D.S., S.A.M., R.C.K., K.J.R. and K.C.K. provided the resources for the study, including provision of study materials, patients, laboratory samples, instrumentation, computing resources and other analysis tools. S.L.H., F.L.B., X.A., J.S.S., T.C.N., G.D.C., T.J., S.D.L., L.T.G., K.A.B., S.L.R., S.A.M., R.C.K., K.J.R. and K.C.K. were responsible for data curation, including management activities to annotate, scrub data and maintain research data for initial use and later reuse. M.S.E.S., S.A.M., R.C.K., K.C.K., V.D.C. and K.J.R. were responsible for supervision, overseeing and providing leadership for the planning and execution of the research activities, including mentorship external to the core team. K.C.K., S.A.M., R.C.K., V.D.C. and K.J.R. were responsible for acquisition of the financial support for the project leading to this publication.

Competing interests

M.S.E.S. has served as a consultant for Niji Corp for unrelated work. N.P.D. is on the scientific advisory board for Sentio Solutions, Inc. and Circular Genomics, Inc. Over the past 3 years, D.A. Pizzagalli has received consulting fees from Boehringer Ingelheim, Compass Pathways, Engrail Therapeutics, Neumora Therapeutics (former BlackThorn Therapeutics), Neurocrine Biosciences, Neuroscience Software, Otsuka Pharmaceuticals, Sage Therapeutics and Takeda Pharmaceuticals; honoraria from the Psychonomic Society and the American Psychological Association (for editorial work) and Alkermes, and research funding from the Bird Foundation, Brain and Behavior Research Foundation, DARPA, Millennium Pharmaceuticals and the National Institute of Mental Health. In addition, he has received stock options from Compass Pathways, Engrail Therapeutics, Neumora Therapeutics (former BlackThorn Therapeutics) and Neuroscience Software. T.C.N. has received research support from NIH, VA and Rainwater Charitable Foundation, and consulting income from Jazz Pharmaceuticals. In the past 3 years, G.D.C. has received research funding from the NSF, NIH and LifeBell AI, and unrestricted donations from AliveCor Inc., Amazon Research, the Center for Discovery, the Gates Foundation, Google, the Gordon and Betty Moore Foundation, MathWorks, Microsoft Research, Nextsense Inc., One Mind Foundation and the Rett Research Foundation. G.D.C. has financial interest in AliveCor Inc. and Nextsense Inc. He also is the CTO of MindChild Medical with significant stock. These relationships are unconnected to the current work. L.T.G. is on the board of the Many Brains Project. Her family also has equity in Intelerad Medical Systems, Inc. S.L.R. reported serving as secretary of the Society of Biological Psychiatry; serving as a board member of Community Psychiatry and Mindpath Health; serving as a board member of National Association of Behavioral Healthcare; serving as secretary and a board member for the Anxiety and Depression Association of America; serving as a board member of the National Network of Depression Centers; receiving royalties from Oxford University Press, American Psychiatric Publishing Inc. and Springer Publishing; and receiving personal fees from the Society of Biological Psychiatry, Community Psychiatry and Mindpath Health, and National Association of Behavioral Healthcare outside the submitted work. C.W.J. has no competing interests related to this work, although he has been an investigator on studies funded by AstraZeneca, Vapotherm, Abbott and Ophirex. S.E.H. has no competing interest related to this work, although in the past 3 years he has received research funding from Aptinyx and Arbor Medical Innovations, and consulting payments from Aptinyx. In the past 3 years, R.C.K. was a consultant for Cambridge Health Alliance, Canandaigua VA Medical Center, Holmusk, Partners Healthcare, Inc., RallyPoint Networks, Inc. and Sage Therapeutics. He has stock options in Cerebral Inc., Mirah, PYM and Roga Sciences. K.C.K.'s research has been supported by the Robert Wood Johnson Foundation, the Kaiser Family Foundation, the Harvard Center on the Developing Child, Stanley Center for Psychiatric Research at the Broad Institute of MIT and Harvard, the National Institutes of Health, One Mind, the Anonymous Foundation and Cohen Veterans Bioscience. She has been a paid consultant for Baker Hostetler, Discovery Vitality and the Department of Justice. She has been a paid external reviewer for the Chan Zuckerberg Foundation, the

University of Cape Town and Capita Ireland. She has had paid speaking engagements in the past 3 years with the American Psychological Association, European Central Bank. Sigmund Freud University–Milan, Cambridge Health Alliance and Coverys. She receives royalties from Guilford Press and Oxford University Press. S.A.M. has served as a consultant for Walter Reed Army Institute for Research, Arbor Medical Innovations and BioXcel Therapeutics, Inc. K.J.R. has performed scientific consultation for Bioxcel, Bionomics, Acer and Jazz Pharma; serves on scientific advisory boards for Sage, Boehringer Ingelheim, Senseye and the Brain Research Foundation; and has received sponsored research support from Alto Neuroscience. The other authors declare no competing interests.

Additional information

Supplementary information The online version contains supplementary material available at https://doi.org/10.1038/s44220-024-00377-0.

Correspondence and requests for materials should be addressed to Mohammad S. E. Sendi.

Peer review information *Nature Mental Health* thanks Mayuresh Korgaonkar, Yuan Zhong and the other, anonymous, reviewer(s) for their contribution to the peer review of this work.

Mohammad S. E. Sendi[1,2,3,4] ✉, Zening Fu[4], Nathaniel G. Harnett[1,2], Sanne J. H. van Rooij[5], Victor Vergara[4,6], Diego A. Pizzagalli[1,2], Nikolaos P. Daskalakis[1,2,3], Stacey L. House[7], Francesca L. Beaudoin[8,9], Xinming An[10], Thomas C. Neylan[11], Gari D. Clifford[12,13], Tanja Jovanovic[14], Sarah D. Linnstaedt[10], Laura T. Germine[2,15,16], Kenneth A. Bollen[17], Scott L. Rauch[2,15,18], John P. Haran[19], Alan B. Storrow[20], Christopher Lewandowski[21], Paul I. Musey Jr.[22], Phyllis L. Hendry[23], Sophia Sheikh[23], Christopher W. Jones[24], Brittany E. Punches[25,26], Robert A. Swor[27], Nina T. Gentile[28], Vishnu P. Murty[29], Lauren A. Hudak[30], Jose L. Pascual[31,32], Mark J. Seamon[32,33], Erica Harris[34], Anna M. Chang[35], Claire Pearson[36], David A. Peak[37], Roland C. Merchant[38], Robert M. Domeier[39], Niels K. Rathlev[40], Brian J. O'Neil[41], Paulina Sergot[42], Leon D. Sanchez[38,43], Steven E. Bruce[44], John F. Sheridan[45,46], Steven E. Harte[47,48], Ronald C. Kessler[49], Karestan C. Koenen[50], Samuel A. McLean[51,52], Jennifer S. Stevens[5], Vince D. Calhoun[4,53] & Kerry J. Ressler[1,2]

[1]Division of Depression and Anxiety, McLean Hospital, Belmont, MA, USA. [2]Department of Psychiatry, Harvard Medical School, Boston, MA, USA. [3]Stanley Center for Psychiatric Research, Broad Institute of MIT and Harvard, Cambridge, MA, USA. [4]Tri-Institutional Center for Translationaal Research in Neuroimaging and Data Science (TReNDS), Georgia State University, Georgia Institute of Technology and Emory University, Atlanta, GA, USA. [5]Department of Psychiatry and Behavioral Sciences, Emory University School of Medicine, Atlanta, GA, USA. [6]Blue Halo, Albuquerque, NM, USA. [7]Department of Emergency Medicine, Washington University School of Medicine, St Louis, MO, USA. [8]Department of Epidemiology, Brown University, Providence, RI, USA. [9]Department of Emergency Medicine, Brown University, Providence, RI, USA. [10]Institute for Trauma Recovery, Department of Anesthesiology, University of North Carolina, Chapel Hill, NC, USA. [11]Departments of Psychiatry and Neurology, University of California, San Francisco, CA, USA. [12]Department of Biomedical Informatics, Emory University School of Medicine, Atlanta, GA, USA. [13]Department of Biomedical Engineering, Georgia Institute of Technology and Emory University, Atlanta, GA, USA. [14]Department of Psychiatry and Behavioral Neurosciences, Wayne State University, Detroit, MI, USA. [15]Institute for Technology in Psychiatry, McLean Hospital, Belmont, MA, USA. [16]The Many Brains Project, Belmont, MA, USA. [17]Department of Psychology and Neuroscience and Department of Sociology, University of North Carolina, Chapel Hill, NC, USA. [18]Department of Psychiatry, McLean Hospital, Belmont, MA, USA. [19]Department of Emergency Medicine, University of Massachusetts Chan Medical School, Worcester, MA, USA. [20]Department of Emergency Medicine, Vanderbilt University Medical Center, Nashville, TN, USA. [21]Department of Emergency Medicine, Henry Ford Health System, Detroit, MI, USA. [22]Department of Emergency Medicine, Indiana University School of Medicine, Indianapolis, IN, USA. [23]Department of Emergency Medicine, University of Florida College of Medicine, Jacksonville, FL, USA. [24]Department of Emergency Medicine, Cooper Medical School of Rowan University, Camden, NJ, USA. [25]Department of Emergency Medicine, Ohio State University College of Medicine, Columbus, OH, USA. [26]College of Nursing, Ohio State University, Columbus, OH, USA. [27]Department of Emergency Medicine, Oakland University William Beaumont School of Medicine, Rochester, MI, USA. [28]Department of Emergency Medicine, Lewis Katz School of Medicine, Temple University, Philadelphia, PA, USA. [29]Department of Psychology, Temple University, Philadelphia, PA, USA. [30]Department of Emergency Medicine, Emory University School of Medicine, Atlanta, GA, USA. [31]Department of Surgery, Department of Neurosurgery, University of Pennsylvania, Philadelphia, PA, USA. [32]Perelman School of Medicine, University of Pennsylvania, Philadelphia, PA, USA. [33]Department of Surgery, Division of Traumatology, Surgical Critical Care and Emergency Surgery, University of Pennsylvania, Philadelphia, PA, USA. [34]Department of Emergency Medicine, Einstein Medical Center, Philadelphia, PA, USA. [35]Department of Emergency Medicine, Jefferson University Hospitals, Philadelphia, PA, USA. [36]Department of Emergency Medicine, Wayne State University and Ascension St John Hospital, Detroit, MI, USA. [37]Department of Emergency Medicine, Massachusetts General Hospital, Boston, MA, USA. [38]Department of Emergency Medicine, Brigham and Women's Hospital, Boston, MA, USA. [39]Department of Emergency Medicine, Trinity Health–Ann Arbor, Ypsilanti, MI, USA. [40]Department of Emergency Medicine, University of Massachusetts Medical School–Baystate, Springfield, MA, USA. [41]Department of Emergency Medicine, Wayne State University and Detroit Receiving Hospital, Detroit, MI, USA. [42]Department of Emergency Medicine, McGovern Medical School at UTHealth, Houston, TX, USA. [43]Department of Emergency Medicine, Harvard Medical School, Boston, MA, USA. [44]Department of Psychological Sciences, University of Missouri, St Louis, MO, USA. [45]Division of Biosciences, Ohio State University College of Dentistry, Columbus, OH, USA. [46]Institute for Behavioral Medicine Research, OSU Wexner Medical Center, Columbus, OH, USA. [47]Department of Anesthesiology, University of Michigan Medical School, Ann Arbor, MI, USA.

[48]Department of Internal Medicine–Rheumatology, University of Michigan Medical School, Ann Arbor, MI, USA. [49]Department of Health Care Policy, Harvard Medical School, Boston, MA, USA. [50]Department of Epidemiology, Harvard T. H. Chan School of Public Health, Harvard University, Boston, MA, USA. [51]Department of Emergency Medicine, University of North Carolina, Chapel Hill, NC, USA. [52]Institute for Trauma Recovery, Department of Psychiatry, University of North Carolina, Chapel Hill, NC, USA. [53]Department of Electrical and Computer Engineering, Georgia Institute of Technology, Atlanta, GA, USA.
✉e-mail: msendi@mclean.harvard.edu

nature portfolio

Corresponding author(s): Mohammad S.E. Sendi

Last updated by author(s): 2024.07.10

Reporting Summary

Nature Portfolio wishes to improve the reproducibility of the work that we publish. This form provides structure for consistency and transparency in reporting. For further information on Nature Portfolio policies, see our Editorial Policies and the Editorial Policy Checklist.

Statistics

For all statistical analyses, confirm that the following items are present in the figure legend, table legend, main text, or Methods section.

n/a	Confirmed
☐	☒ The exact sample size (*n*) for each experimental group/condition, given as a discrete number and unit of measurement
☐	☒ A statement on whether measurements were taken from distinct samples or whether the same sample was measured repeatedly
☐	☒ The statistical test(s) used AND whether they are one- or two-sided *Only common tests should be described solely by name; describe more complex techniques in the Methods section.*
☐	☒ A description of all covariates tested
☐	☒ A description of any assumptions or corrections, such as tests of normality and adjustment for multiple comparisons
☐	☒ A full description of the statistical parameters including central tendency (e.g. means) or other basic estimates (e.g. regression coefficient) AND variation (e.g. standard deviation) or associated estimates of uncertainty (e.g. confidence intervals)
☐	☒ For null hypothesis testing, the test statistic (e.g. *F*, *t*, *r*) with confidence intervals, effect sizes, degrees of freedom and *P* value noted *Give P values as exact values whenever suitable.*
☒	☐ For Bayesian analysis, information on the choice of priors and Markov chain Monte Carlo settings
☒	☐ For hierarchical and complex designs, identification of the appropriate level for tests and full reporting of outcomes
☐	☒ Estimates of effect sizes (e.g. Cohen's *d*, Pearson's *r*), indicating how they were calculated

Our web collection on statistics for biologists contains articles on many of the points above.

Software and code

Policy information about availability of computer code

Data collection	The Mindstrong Discovery™ app was used to collect clinical data. It was downloaded from the App Store (iOS users) or from Google Play (Android users) onto the participant's smartphone.
Data analysis	The code used for preprocessing and dFNC calculation are available at https://trendscenter.org/software/. Also, statistical parametric mapping or SPM 12 is available at https://www.fil.ion.ucl.ac.uk/spm/.The Neuromark framework and the Neuromark_fMRI_1.0 template have been made available and incorporated into the Group ICA Toolbox (GIFT v4.0.5.14: https://trendscenter.org/software/gift/). Users worldwide can now directly download and utilize these resources. The chord graphs are generated using the NiChord toolbox in Python (https://github.com/paulcbogdan/NiChord). The General Linear Model (GLM) code in MATLAB is available in https://www.mathworks.com/help/stats/fitglm.html.

For manuscripts utilizing custom algorithms or software that are central to the research but not yet described in published literature, software must be made available to editors and reviewers. We strongly encourage code deposition in a community repository (e.g. GitHub). See the Nature Portfolio guidelines for submitting code & software for further information.

Data

Policy information about availability of data

All manuscripts must include a data availability statement. This statement should provide the following information, where applicable:

- Accession codes, unique identifiers, or web links for publicly available datasets
- A description of any restrictions on data availability
- For clinical datasets or third party data, please ensure that the statement adheres to our policy

The data and research tools used in the preparation of this manuscript were sourced from the National Institute of Mental Health (NIMH) Data Archive (NDA). The NDA is a collaborative informatics system established by the National Institutes of Health to provide a national resource that supports and accelerates mental health research. The specific dataset used can be accessed via the NIMH Data Archive Digital Object Identifier (DOI): 10.15154/zwyn-rb26. We commit to making the materials, data, code, and associated protocols promptly available without undue qualifications upon reasonable request.

Research involving human participants, their data, or biological material

Policy information about studies with human participants or human data. See also policy information about sex, gender (identity/presentation), and sexual orientation and race, ethnicity and racism.

Reporting on sex and gender	Biological sex assigned at birth, as self-reported by participants, is included in the analysis presented in this manuscript. Our study sample comprises 65.82% women. We conducted analyses to explore the impact of biological sex on our findings. The rationale for including and analyzing data across different sexes is detailed in the manuscript.
Reporting on race, ethnicity, or other socially relevant groupings	Race and ethnicity, along with marital status, education level, and income, are self-reported and detailed in the manuscript. This self-reported method ensures the inclusion of comprehensive demographic information, reflecting the diversity of the study sample. The manuscript presents specific data on the distribution of race and ethnicity, underscoring the inclusiveness and self-reported accuracy of the demographic details collected.
Population characteristics	Refer to the Behavioral & Social Sciences study design section above
Recruitment	Participants were eligible for this study if they had been exposed to trauma, specifically defined as experiencing a traumatic event that required evaluation in an Emergency Department (ED). Research assistants (RAs), stationed at participating EDs, approached potential participants within 72 hours of their traumatic event. The RAs provided a detailed overview of the study, including the general nature of the research, expectations for participation, and its voluntary nature. They also discussed the potential risks and benefits associated with participation before seeking written informed consent. It is acknowledged that there is a risk of self-selection bias, as individuals who chose not to participate might have done so for various reasons, potentially influencing the study's demographic and psychological diversity.
Ethics oversight	This study was carried out in strict adherence to ethical standards and received approval from the Institutional Review Board (IRB) at the University of North Carolina (IRB no. 1707-03) on May 12, 2017. This approval covered multiple research sites, with additional sites either entering into reliance agreements or conducting their own parallel IRB reviews. All participants provided written informed consent before taking part in the study. To ensure participant safety and ethical oversight, an independent medical monitor was appointed to evaluate and approve the procedures for managing any cases of clinical deterioration reported by participants or identified by the study staff. This monitor also reviewed detailed reports of participant interactions, which were prepared by experienced clinicians.

Note that full information on the approval of the study protocol must also be provided in the manuscript.

Field-specific reporting

Please select the one below that is the best fit for your research. If you are not sure, read the appropriate sections before making your selection.

☐ Life sciences ☒ Behavioural & social sciences ☐ Ecological, evolutionary & environmental sciences

For a reference copy of the document with all sections, see nature.com/documents/nr-reporting-summary-flat.pdf

Behavioural & social sciences study design

All studies must disclose on these points even when the disclosure is negative.

Study description	The data analyzed in this study were derived from the multisite AURORA study, conducted in emergency departments (EDs) across the United States. The AURORA study is a landmark research initiative designed to advance understanding, prevention, and recovery strategies for individuals exposed to traumatic events. Trauma-exposed civilians presenting at one of 29 participating EDs were enrolled in this extensive longitudinal study. Approximately 3,000 participants contributed clinical data at multiple time points: 2 weeks (WK2), 4 weeks (WK4), 3 months (M3), 6 months (M6), and 12 months (M12), as depicted in Fig. 1A. Furthermore, neuroimaging data were obtained at WK2 from around 400 participants at five scanning sites: Atlanta (Georgia), Belmont (Massachusetts), Philadelphia (Pennsylvania), St. Louis (Missouri), and Detroit (Michigan). Recruitment occurred from September

2017 to June 2021, with the final psychometric data release (Freeze 4) completed on September 22, 2021. For a comprehensive description of the study design, please refer to McLean et al. (2020)

Research sample

The chosen study sample was selected to ensure a comprehensive and representative analysis of trauma-exposed individuals presenting to the Emergency Department (ED) within 72 hours of a traumatic event. The inclusion of patients aged 18–75 years allows the study to capture a broad spectrum of adult trauma experiences while minimizing recall bias by focusing on the acute phase of trauma exposure. This time frame is critical for assessing early physiological and psychological responses, which are key to understanding the immediate aftermath of trauma and its potential long-term effects.

The sample comprises a diverse group of participants, enhancing the generalizability of the findings. The average age of the sample is approximately 34.55 years, with 34.18% males and 65.82% females, reflecting a realistic gender distribution in trauma studies. The racial composition includes Black participants (47.64%), White participants (30.91%), Hispanic participants (15.27%), and individuals categorized as other races (5.45%), ensuring that the study addresses the experiences of racial and ethnic minorities, who are often underrepresented in research.

Socioeconomic diversity is another strength of this sample, with the majority of participants earning below $35,000 annually. This income distribution allows for the exploration of socioeconomic factors in trauma recovery, which are critical for developing equitable intervention strategies. The average educational attainment of approximately 15 years ensures the inclusion of individuals with a range of educational backgrounds.

The types of trauma experienced by the participants further underscore the representativeness of the sample. Motor vehicle collisions, the most common trauma type, account for 71.64% of cases, mirroring a frequent cause of ED visits in the general population. The inclusion of other trauma types—such as physical assaults, falls, non-motorized collisions, and animal-related incidents—provides a heterogeneous dataset for studying diverse trauma experiences. Less frequent but significant events, including burns, sexual assaults, and incidents involving traumatic stress exposure to multiple people, broaden the scope of the study, enabling the examination of unique trauma responses.

Overall, this sample was chosen to capture the variability in demographic, socioeconomic, and trauma-specific factors, ensuring that the findings are broadly applicable. The diversity within the sample allows for nuanced analyses of how individual characteristics and trauma types influence recovery trajectories, supporting the study's aim to develop insights and interventions that can benefit a wide range of trauma-exposed populations.

Sampling strategy

Patients presenting to participating Emergency Department (ED) sites within 72 hours of experiencing trauma were screened for eligibility to participate in the AURORA study. The initial goal was to enroll 5,000 participants, with the study design allowing for adaptive sampling of specific trauma subsamples and necessary adjustments throughout the study duration to meet its objectives. The study wrapped up in June 2021, concluding with a final sample of 2,943 participants who had follow-up data available. Those recruited at one of the ED locations linked to the AURORA study and directed to one of five 'deep phenotyping' sites were invited to undergo MRI scans. These scans took place either in the morning or afternoon, roughly two weeks after the traumatic incident (i.e., WK2). Following extensive preprocessing and rigorous quality checks, data from 275 participants were ultimately included in our analysis. Power and sample size calculations were performed a priori in October 2019 using the Correlation Sample Size tool available at sample-size.net. These calculations were based on effect size estimates from a previous study conducted in the Emergency Department at Emory University, which investigated posttraumatic stress disorder. The relevance of these effect sizes to our current analysis stems from the use of identical fMRI tasks and MRI acquisition sequences in both the AURORA study and the Emory ED study. Given a prior study effect size of Cohen's f2 around 0.15, the minimum required sample size to achieve a power of 0.95 with an alpha level of 0.0033 is 90. The alpha was set at 0.0033 to adjust for multiple comparisons involving 15 tests.

Data collection

Emergency Department (ED) assessments were carried out by trained research assistants without any restrictions on the presence of others, including hospital staff, family, or friends. Although the study did not involve specific experimental conditions or defined hypotheses, the research assistants were informed about the overarching goals of the study.Participants installed a designated smartphone app on their Android or iOS devices. Follow-up surveys were conducted at 2 weeks, 8 weeks, 3 months, 6 months, and 12 months post-initial evaluation, using either web-based or phone-based self-report methods. Additionally, a select group of participants was invited to undergo an MRI scan two weeks after joining the study in the ED.

Timing

The first time point for data collection was within 72 hours of trauma exposure in the ED. Follow-up assessments were completed 2-weeks, 8-weeks, 3-months, 6-months, and 12-months after initial evaluation. For this manuscript, data collected in the ED, at 2 weeks, 8 weeks, 3 months, 6 months, and 12 months following trauma exposure were used.

Data exclusions

The study eventually included 2,772 AURORA participants with clinical item-level data, recruited between September 2017 and June 2021, marking the final data freeze for psychometric release (Freeze 4.0 dataset released at 22/09/2021). Participants recruited at one of the Emergency Department (ED) locations for the AURORA study, which directed participants to one of five 'deep phenotyping' sites, were invited to undergo MRI scans. These scans were conducted either in the morning or afternoon, approximately two weeks following the traumatic event (i.e., WK2). After thorough preprocessing and quality checks, data from 275 participants were included in our study.

Non-participation

Randomization

The study was observational and participants were not allocated to groups.

Reporting for specific materials, systems and methods

We require information from authors about some types of materials, experimental systems and methods used in many studies. Here, indicate whether each material, system or method listed is relevant to your study. If you are not sure if a list item applies to your research, read the appropriate section before selecting a response.

Materials & experimental systems

n/a	Involved in the study
☒	☐ Antibodies
☒	☐ Eukaryotic cell lines
☒	☐ Palaeontology and archaeology
☒	☐ Animals and other organisms
☒	☐ Clinical data
☒	☐ Dual use research of concern
☒	☐ Plants

Methods

n/a	Involved in the study
☒	☐ ChIP-seq
☒	☐ Flow cytometry
☐	☒ MRI-based neuroimaging

Magnetic resonance imaging

Experimental design

Design type	resting-state fMRI
Design specifications	No task fMRI were included in our current study
Behavioral performance measures	No task fMRI were included in our current study

Acquisition

Imaging type(s)	Functional
Field strength	3T
Sequence & imaging parameters	Site 1 (Emory) Siemens TIM 3T Trio (12-channel head coil) T1-weighted: TR = 2530ms, TEs = 1.74/3.6/ 5.46/7.32ms, TI = 1260ms, flip angle = 7, FOV = 256mm, slices = 176, Voxel size = 1mm x 1mm x 1mm Functional MRI: TR = 2360ms, TE = 30ms, flip angle = 70, FOV = 212mm, slices = 44, Voxel size = 3mm x 2.72mm x 2.72mm, 0.5 mm gap Site 2 (McLean) Siemens TIM 3T Trio (12-channel head coil) T1-weighted: TR = 2530ms, TEs = 1.74/3.6/ 5.46/7.32ms, TI = 1260ms, flip angle = 7, FOV = 256mm, slices = 176, Voxel size = 1mm x 1mm x 1mm Functional MRI: TR = 2360ms, TE = 30ms, flip angle = 70, FOV = 212mm, slices = 44, Voxel size = 3mm x 3mm x 3mm, 0.5 mm gap Site 3 (Wayne) Siemens Magnetom 3T PRISMA (20-channel head coil) T1-weighted: TR = 2300ms, TE = 2.96ms, TI = 900ms, flip angle = 9, FOV = 256mm, slices = 176, Voxel size = 1.2mm x 1.0mm x 12mm Functional MRI: TR = 2360ms, TE = 29ms, flip angle = 70, FOV = 212mm, slices = 44, Voxel size = 3mm x 2.72mm x 2.72mm, 0.5 mm gap Site 4 (Temple) Siemens 3T Verio (12-channel head coil) T1-weighted: TR = 2530ms, TEs = 1.74/3.65/ 5.51/7.72ms, TI = 1260ms, flip angle = 7, FOV = 256mm, slices = 176, Voxel size = 1mm x 1mm x 1mm Functional MRI: TR = 2360ms, TE = 30ms, flip angle = 70, FOV = 212mm, slices = 42, Voxel size = 3mm x 2.72mm x 2.72mm, 0.5 mm gap Site 5 (Wash U) Siemens Magnetom 3T PRISMA (20-channel head coil) T1-weighted: TR = 2300ms, TE = 2.98ms, TI = 900ms, flip angle = 9, FOV = 256mm, slices = 176, Voxel size = 1.2mm x 1.0mm x 12mm Functional MRI: TR = 2360ms, TE = 29ms, flip angle = 90, FOV = 210mm, slices = 44, Voxel size = 3mm x 3mm x 2.5mm, 0.5 mm gap
Area of acquisition	Whole brain scan was used

Diffusion MRI ☐ Used ☒ Not used

Preprocessing

Preprocessing software	We adjusted for variations in image acquisition times across slices using the default slice timing routines from statistical parametric mapping (SPM12, available at https://www.fil.ion.ucl.ac.uk/spm/). The slice captured mid-sequence was used as

the reference. Subsequently, corrections for the subject's head movements were made using rigid body alignment, and estimates were made for both 3-dimensional translations and rotations of the brain. The imaging data were then resampled to a 3 × 3 × 3 mm^3 resolution and spatially normalized to the Montreal Neurological Institute (MNI) space using the echo-planar imaging (EPI) template from the SPM toolbox. Following this, the fMRI images underwent smoothing with a Gaussian kernel set at a full width at half maximum (FWHM) of 6 mm.

We utilized a hybrid Neuromark framework to identify significant networks for each participant. The Neuromark framework utilizes templates developed from two extensive datasets: the Human Connectome Project (HCP: https://www.humanconnectome.org/study/hcp-young-adult/document/1200-subjects-data-release, with 823 subjects after selection) and the Genomics Superstruct Project (GSP: https://dataverse.harvard.edu/dataverse/GSP, with 1005 subjects after selection). This approach has been effectively used in numerous studies to identify a range of brain imaging markers across various brain disorders. Further details on the creation of these templates are available in our prior Neuromark publication.

The Neuromark template includes 53 independent components (ICs), organized into seven functional networks based on anatomical and functional insights. These networks are the subcortical network (SCN), auditory network (ADN), sensorimotor network (SMN), visual network (VSN), cognitive control network (CCN), default-mode network (DMN), and cerebellar network (CBN). All 53 ICs and their associations are detailed in Supplementary Table 3. We applied these predefined templates (available in the Neuromark_fMRI_1.0 template on GIFT at http://trendscenter.org/software/gift and the TReNDS website at http://trendscenter.org/data) to conduct a comprehensive automated ICA analysis using GIFT software. This analysis included: 1) removing linear, quadratic, and cubic trends; 2) performing multiple regression analyses on the six alignment parameters and their temporal derivatives; 3) despiking to address detected outliers; and 4) implementing a low-pass filter with a cut-off frequency at 0.15Hz to eliminate noise and artifacts.

Dynamic functional network connectivity (dFNC) across the entire brain was calculated using a sliding window method. We employed a tapered window formed by convolving a rectangular window (20 TRs or 47.2 seconds) with a Gaussian distribution ($\sigma = 3$) to precisely localize the dataset at each time point. For each window, Pearson correlation was used to measure the functional network connectivity among all 53 independent components (ICs). This computation generated a symmetric 53×53 matrix, reflecting the connectivity between every pair of ICs, amounting to 1378 connectivity features per window due to the combinatorial arrangements of the 53 ICs. Subsequently, the dFNCs from each participant were compiled into a (C × C × T) array, where C represents the 53 ICs and T denotes 210 time points, effectively mapping the temporal evolution of connectivity changes among the ICs.

Normalization: Non-linear

Normalization template: EPI template

Noise and artifact removal: After obtaining the subject-specific time courses, we did additional post-processing on the time courses to remove the noise, including 1) detrending linear, quadratic, and cubic trends, 2) multiple regression of the 6 realignment parameters and their derivatives, 3) removal of detected outliers, and 4) low-pass filtering with a cutoff frequency of 0.15 Hz. Our filtering was performed on the TC of ICs, not on the voxel-based fMRI data because we want to retain more information on fMRI for ICA decomposition.

Volume censoring: An overall motion threshold was implemented for any run with >15% of volumes with more than 1mm framewise displacement in order to handle cases in which motion was likely too high for effective ICA correction.

Statistical modeling & inference

Model type and settings: We utilized a General Linear Model (GLM) to investigate the relationship between dynamic functional network connectivity (dFNC) variables and PCL-5 scores, incorporating data from all participants. Our analysis accounted for covariates including age, sex at birth, years of education, income, employment status, marital status, scanning site, type of trauma, and percentile ADI. In our sex-stratified models, we omitted sex from the list of covariates

Effect(s) tested: The model tested the hypothesis that variations in dynamic functional network connectivity (dFNC) are associated with changes in PCL-5 scores, adjusting for covariates such as age, years of education, income, employment status, marital status, scanning site, type of trauma, and ADI. The analysis specifically examined whether these associations differ by sex, excluding sex as a covariate in sex-stratified models.

Specify type of analysis: ☒ Whole brain ☐ ROI-based ☐ Both

Statistic type for inference (See Eklund et al. 2016): We concentrated on assessing the functional connectivity across all brain regions

Correction: FDR

Models & analysis

n/a	Involved in the study
☐	☒ Functional and/or effective connectivity
☒	☐ Graph analysis
☐	☒ Multivariate modeling or predictive analysis

Functional and/or effective connectivity	Pearson Correlation
Multivariate modeling and predictive analysis	In our analysis, dFNC variables, including the occupancy rate of three identified states, were used as independent variables. We employed PCL-5 scores from week 2, week 8, month 3, month 6, and month 12 post-trauma as the dependent variables. Our analysis accounted for covariates such as age, sex at birth, years of education, income, employment status, marital status, scanning site, type of trauma, and percentile ADI. In our sex-stratified models, we excluded sex from the list of covariates.